Toward the realization of a primary low-pressure standard using a superconducting microwave resonator

P. Gambette, R M Gavioso, D. Madonna Ripa, M D Plimmer, F. Sparasci, L. Pitre

Toward the realization of a primary low-pressure standard using a superconducting microwave resonator

P. Gambette,[1] R.M. Gavioso,[2] D. Madonna Ripa,[2] M.D. Plimmer,[1] F. Sparasci,[1] and L. Pitre[1]

[1)]*LNE-Cnam, 61 rue du Landy, F93210 La Plaine-St Denis, France*

[2)]*Istituto Nazionale di Ricerca Metrologica (INRiM), Strada delle Cacce 91, 10135 Torino, Italy*

(*Electronic mail: pascal.gambette@cnam.fr)

(Dated: 1 February 2023)

We describe a primary gas pressure standard based on the measurement of the refractive index of helium gas using a microwave resonant cavity in the range between 500 Pa and 20 kPa. To operate in this range, the sensitivity of the microwave refractive index manometer (MRGM) to low pressure variations is substantially enhanced by a niobium coating of the resonator surface which becomes superconducting at temperatures below 9 K, allowing one to achieve a frequency resolution of about 0.3 Hz at 5.2 GHz corresponding to a pressure resolution below 3 mPa at 20 Pa. The determination of helium pressure requires precise thermometry but is favoured by the remarkable accuracy achieved by *ab initio* calculations of the thermodynamic and electromagnetic properties of the gas. The overall standard uncertainty of the MRGM is estimated to be of the order of 0.04 %, corresponding to 0.2 Pa at 500 Pa and 8.1 Pa at 20 kPa, with major contributions from thermometry and the repeatability of microwave frequency measurements. A direct comparison of the pressures realized by the MRGM with the reference provided by a traceable quartz transducer shows relative pressure differences between 0.025 % at 20 kPa and −1.4 % at 500 Pa.

I. INTRODUCTION

In 1998, Moldover proposed that a thermodynamic standard of pressure could be based on the measurement of an intensive quantity such as the permittivity or refractivity of a gas[1,2]. In the following two decades, this metrological concept has been well demonstrated, becoming increasingly competitive with pressure balances and liquid column manometers in terms of both accuracy and flexibility of use.

Much of the progress in this field must be credited to the increased accuracy of the *ab initio* calculation of the electromagnetic and thermodynamic properties of gases from fundamental constants, quantum mechanics, and statistical mechanics. The properties of dilute helium[3–5] can now be calculated with much lower uncertainty that they can be measured. Similar calculations have significantly reduced the uncertainty of more refractive gases, such as neon[6], argon[7], and nitrogen[8], which may be useful for low-pressure metrology.

Among the alternatives to mechanical pressure standards, there are gas refractometers using fixed- or variable-length optical cavities whose design is derived from apparatuses developed to measure the density of air[9,10]. A recent review[11] of optical pressure standards discusses various methods and the perspectives of their further improvement. Notable achievements include the use of dual Fabry-Perot cavities to determine the refractive index of nitrogen[12], and the realization of a pressure transfer standard with an estimated standard uncertainty between 10 ppm and 5 ppm in the range between 100 Pa and 180 kPa respectively[13].

Some open technical problems currently limit the performance and range of application of these methods. In particular, the helium used to estimate pressure distortion errors can diffuse into the ultra-low expansion glass cavity spacers. There are also various long- and short-term dimensional instabilities.

These issues do not affect gas-based primary thermometry methods based on capacitors or microwave resonant cavities, which have been successfully used to realize primary pressure standards in the MPa range.

In particular, refractive index gas thermometry (RIGT)[14] was previously used to implement a He-based primary pressure standard[15] with a relative standard pressure uncertainty $u_r(p)$ within 9×10^{-6} between 0.8 MPa and 7 MPa. More recently, dielectric constant gas thermometry (DCGT)[9] techniques have progressively[16,17] reduced the overall uncertainty of a capacitance pressure standard to $u_r(p) = 2.2\times10^{-6}$ at 7 MPa. However, the range of application of these gas-thermometry methods is normally limited to above 100 kPa by the resolution of relative capacitance or resonance frequency measurements.

In this context, we describe the basic design features of a prototype copper microwave resonator whose sensitivity to small variations of the static refractivity of He is enhanced by a niobium coating of the internal cavity that becomes superconducting at temperatures below 9 K. The corresponding reduction of resistive losses enhances the quality factor of the microwave resonances, leading to a significant extension - by nearly three orders of magnitude - of the range where precise measurements of the refractive index of He may be used to implement a primary pressure standard.

We evaluate the metrological performance of the new standard, dubbed microwave refractive gas manometry (MRGM), by obtaining measurements at pressures between 500 Pa and 20 kPa at temperatures between 5 K and 9 K. We consider the relevant corrections to the measured resonance frequencies as well as other contributions to the uncertainty budget, and we test the validity of our model comparing the pressures resulting from the MRGM measurements to the readings of a reference calibrated quartz transducer.

II. MEASUREMENT PRINCIPLE

Many pressure transducers and standards work by detecting the mechanical action of pressure on the surface of an artefact. In this work, we rely instead on a thermodynamic definition of pressure by measuring the density-dependent refractive index of a sample of gas maintained at a constant temperature within a microwave cavity.

The ratio of frequencies for an evacuated and gas-filled resonator yields to a first approximation the value of refractive index $n(p,T)$, which depends only on pressure p and temperature T. Refractive index measurements thus provide a way to measure either pressure or temperature if the other quantity is known. In constant-pressure refractive index gas thermometry[18] (RIGT), the measurement of n at a known pressure p is used to determine the temperature T. Conversely, the present manometer deduces pressure from the refractive index measured at a well-defined temperature.

A. Relation between refractive index, pressure, and temperature

The refractive index n of a gaseous medium is defined as

$$n^2 = \varepsilon_r \mu_r, \qquad (1)$$

where both the relative dielectric permittivity ε_r and the relative magnetic permeability μ_r are functions of p and T derived as follows. At a temperature T, the pressure of an ideal gas is proportional to the amount-of-substance density ρ_N

$$p = \rho_N kT \qquad (2)$$

where k is the Boltzmann constant. On a molar basis, the ideal equation of state becomes

$$p = \rho_m RT, \qquad (3)$$

where ρ_m is the molar density

$$\rho_m = \frac{\rho_N}{N_A}, \qquad (4)$$

R is the molar gas constant

$$R = kN_A, \qquad (5)$$

and N_A is the Avogadro constant. Notably, the values of k, N_A, and hence R, were fixed in 2019 exactly by the redefinition of the International System of Units (SI).

To describe real gases, as required for accurate gas metrology, a virial equation of state is needed:

$$p = \rho_m RT(1 + B(T)\rho_m + C(T)\rho_m^2 + \cdots). \qquad (6)$$

where $B(T)$, $C(T)$ are the molar density virial coefficients, which can be measured experimentally or determined by *ab initio* calculations. For many-electron atoms such as argon (Z = 18) or neon (Z = 10), the determination of virial coefficients by experimental means currently provides the lowest uncertainties[20]. For helium, however, the determination by *ab initio* calculations has surpassed the accuracy of experiments[20], which motivated the use of helium-4 as the test gas in the present work.

The electric permittivity is related to the molar density via the Clausius-Mossotti equations:

$$\frac{\varepsilon_r - 1}{\varepsilon_r + 2} = \rho_m(A_\varepsilon + B_\varepsilon(T)\rho_m + C_\varepsilon(T)\rho_m^2 + \cdots). \qquad (7)$$

There is a corresponding expansion for the magnetic permeability

$$\frac{\mu_r - 1}{\mu_r + 2} = \rho_m(A_\mu + \cdots). \qquad (8)$$

where A_ε and A_μ are the static, zero-density limits of the molar electric polarizability and the molar magnetic susceptibility, respectively. The coefficients $B_\varepsilon(T)$ and $C_\varepsilon(T)$ are the dielectric virial coefficients[19]. By combining equations 6,7, 8 and 3, the value of p at a given temperature T can be derived from the measured value of $n(p,T)$ via an iterative calculation.

B.Microwave measurement of the refractive index

Extremely accurate measurements of the refractive index of gases can be obtained using a microwave cavity with a quasi-spherical internal shape[21], where this particular geometry lifts the degeneracy of the modes of a perfect sphere, yielding resolved, precisely measurable resonance curves. Considering, among the eigenfrequencies f_{ln} which satisfy the Maxwell equations in spherical geometry, the triply-degenerate modes with $l = 1$, which are most suitable for precise measurements, we denote as f_{1n} the resonance frequencies of the transverse magnetic modes TM_{1n} investigated in this work.

The refractive index of the gas is determined by measuring the ratio of the resonance frequencies $< f_{1n} + \Delta f_{1n} >_0$ and $< f_{1n} + \Delta f_{1n} >$, respectively measured in vacuum and when the cavity is filled with gas at pressure p

$$n = \frac{<f_{1n}+\Delta f_{1n}>_0[1+\kappa_T(p/3)]}{<f_{1n}+\Delta f_{1n}>} \qquad (9)$$

where the brackets <..> denote the mean of the single components of the triplet, and Δf refers to the perturbation induced by the penetration depth of the electromagnetic field within the cavity wall, and the isothermal compressibility k_T accounts for the mechanical deformation of the cavity under pressure. At the moderate pressures investigated here, the compressibility correction is small and a tabulated estimate[22] for copper $\kappa_T = 7.04 \times 10^{-12}$ Pa^{-1} is sufficiently precise at temperatures below 9 K. In principle, the cavity resonance frequencies must also be corrected for the dimensional change induced by any temperature variation occurring during the measurements. However, between 5 K and 9 K the thermal expansion coefficient α_{th} of copper is extremely small, of the order of 2×10^{-8} K^{-1}, compared to 1.7×10^{-6} K^{-1} at ambient temperature, and nearly temperature independent. Our own precise experimental estimate of α_{th} was obtained by resonance frequency measurements in vacuum by varying the temperature set-point by ±0.5 K.

Compared to other atomic gases, the polarizability of He is the lowest, which limits the sensitivity of our frequency measurements to pressure. With $A_\varepsilon \sim 0.517$ cm^3 mol^{-1}, a variation of the He pressure within the cavity by 1 Pa between 100 Pa to 20 kPa leads to a relative frequency change of -18×10^{-9}.

The frequency resolution of the resonator can be expressed by the following relation[18]

$$\frac{\Delta f}{f} = \frac{1}{A}\frac{1}{Q}\frac{1}{(SNR)}\sqrt{\frac{\tau}{t}} \qquad (10)$$

where A is a dimensionless constant of order unity, Q is the quality factor of the cavity, SNR is the signal-to-noise ratio, τ is the single-measurement time and t is the integration time. The measurement of the cavity resonance frequency has a resolution that is inversely proportional to the quality factor Q [18]. With a quasi-spherical copper microwave cavity used here, the Q is of the order of 2×10^4. A niobium-coated superconducting cavity has a higher Q, as much as 10^{10} at lower temperature[23].

III. EXPERIMENT

A. Microwave resonator

The basic design features of the resonator developed for this experiment derives from the cavities previously developed at LNE-Cnam to perform Acoustic Gas Thermometry[24] and Refractive Index Gas Thermometry[18].

It is composed of two identical copper hemispheres (Figure 1) each of mass about 0.5 kg, assembled to form a triaxial ellipsoid[25] of radii 24.95 mm, 25.00 mm and 25.05 mm. It is internally coated[26,27] with a layer of niobium having mean thickness 3 μm, which becomes superconducting below the critical temperature of 9.2 K. To prevent oxidation of the niobium coating from air, the cavity is maintained either under vacuum, or filled with inert gases throughout the experiment.

Four conical copper plugs have also been coated with niobium for insertion into the quasi-sphere. Two of these plugs serve as holders for straight microwave antennas, made with non-magnetic materials. They are used to excite and detect the transverse magnetic modes (TM_{1n}) of the resonator[25], with the resonance frequencies of the lowest magnetic mode TM_{11} found about 5.2 GHz.

The resonator is suspended in a copper pressure vessel. The other two conical plugs have central holes that allow the free circulation of gas between the pressure vessel and the resonant cavity. Equilibrating the pressure between the inside and outside of the resonator limits mechanical stress.

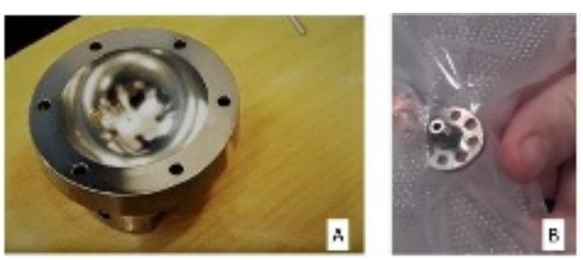

FIG. 1. (A) One of two hemispheres comprising the microwave resonator. The silvery appearance of the internal surface is due to a 3 μm thick layer of niobium deposited over copper. (B) One of the four conical plugs which are used either to provide holding support for antennas or to equilibrate pressure between the internal cavity and the pressure vessel.

B. Experimental set-up

Since the aim of this experiment is to realize a thermodynamic definition of pressure by the measurement of gas density, the temperature must be accurately measured and controlled. Therefore, a custom cryostat has been developed (see Figure 2) whose lowest stage holds the resonator suspended in a pressure vessel. The pressure vessel comprises an indium-sealed, cylindrical copper enclosure with an internal height of 117 mm and an internal diameter of 85 mm. The pressure vessel is suspended in a vacuum chamber comprising an indium-sealed, cylindrical stainless-steel enclosure of an internal height

175 mm and internal diameter 112 mm. Finally, the entire cryostat is inserted into a cylindrical cryogenic storage Dewar (20 L capacity), filled with liquid helium.

The two antenna plugs located in the upper hemisphere bear RF connections to coaxial cables. These cables have a dedicated access to the pressure vessel and the vacuum chamber, passing through liquid helium inside the Dewar. A central stainless-steel tube provides mechanical support to the vacuum chamber and is used for its evacuation, also providing a feed-through passage for wire connections to two heaters and two temperature sensors. One heater and one temperature sensor are fixed in thermal contact with the upper part of the resonator. The second heater and temperature sensor are attached to pressure vessel.

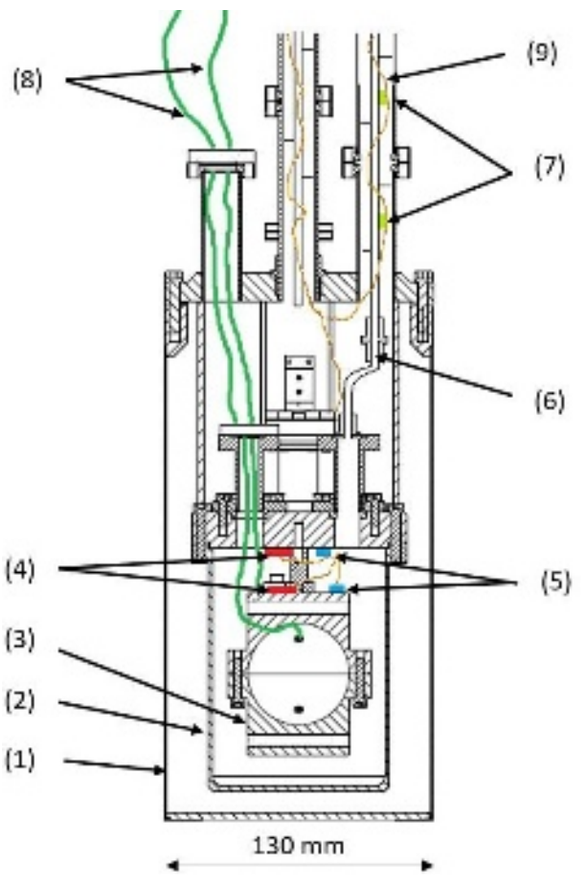

FIG. 2. Cryostat sectional view: (1) Vacuum chamber, (2) Pressure vessel, (3) Superconducting quasi-spherical resonator, (4) Heaters, (5) Cernox^{TM} RTD temperature sensors, (6) Pressure tube, (7) Platinum RTD temperature sensors, (8) Coaxial RF cables, (9) Electrical wiring to temperature sensors and heaters.

Near the cryostat, a pressure generator in a temperature regulated enclosure makes it possible to maintain a stable pressure around a selectable setpoint. It includes two Digiquartz® model 745 pressure sensors[28], respectively used to accurately control the pressure around the setpoint value, to provide a traceable pressure reference for the sake of comparison to the microwave pressure standard. The overall uncertainty of the reference pressure sensor is $u(p)$ = 0.25 Pa at 1 kPa.
The gas line connecting the pressure generator to the pressure vessel is the inner duct of a coaxial tube, where the outer tube is maintained under vacuum, to limit the heat exchange between the gas and the liquid helium bath. Since the pressure measured by the resonator is compared with a standard located over 1 m above it, a precise evaluation of the hydrostatic pressure correction is necessary. For this purpose, five Pt1000 thermometers are fixed at differently spaced locations along the pressure tube to provide the temperature profile needed to calculate the correction.

The helium gas used for the experiment is of purity ≥ 99.9999 % mol, as stated by the manufacturer. Due to the high sensitivity of the refractive index of helium to even trace amounts of impurities, assessing and maintaining the purity of the helium sample is a crucial issue. The gas handling system is entirely made of electropolished stainless steel components and is kept constantly filled with pure helium, to avoid any contamination. In addition, working at 5 K, far below the freezing point of most common impurities, reduces the risk of possible contamination.

To perform microwave measurements, the antennas in the resonator are connected to a vector network analyzer locked to a rubidium clock, providing a stable frequency reference to 1 part in 10^{10} per year. The network analyzer is controlled by a computer to measure the spectrum of the transmission coefficient S_{21} around the resonant frequencies.

Active temperature regulation of the resonator and pressure vessel is achieved by computer control of the power supplied to the corresponding heaters from a current source (Yokogawa GS210-7F28), based on the readings of a resistive temperature sensor by an ohmmeter (Keithley 2002[28]). The pressure vessel and resonator are regulated at the same temperature to reduce thermal gradients across the apparatus.

A simplified, functional schematic diagram of the apparatus is illustrated in Figure 3. A photograph of the whole apparatus is shown in Figure 4.

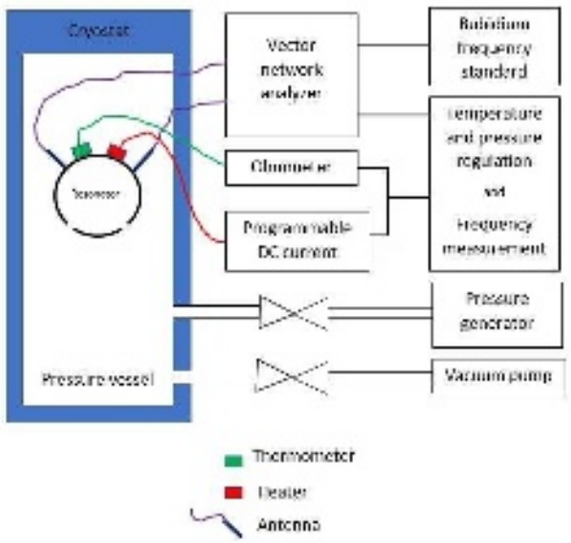

FIG. 3. Schematic of the electronic, pressure and vacuum connections between the cryogenic part of the experiment and the laboratory instrumentation.

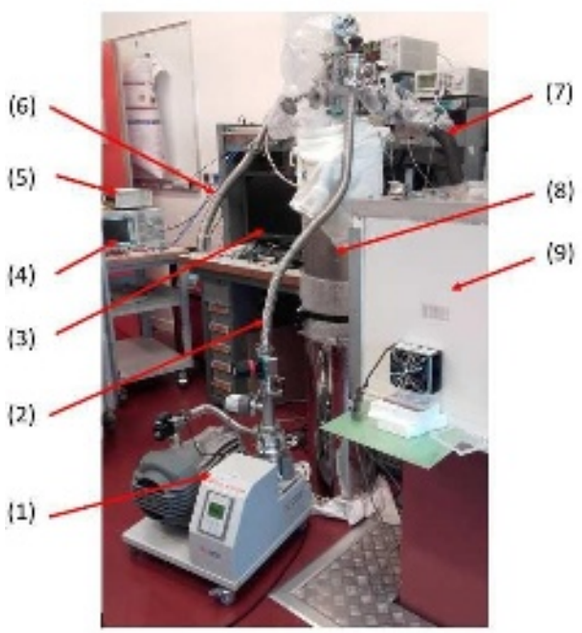

FIG. 4. Experimental setup: (1) Pumping station composed of a turbomolecular pump backed by a dry scroll primary pump (2) Vacuum connection to cryostat, (3) Computers, (4) Vector network analyser connected to the microwave resonator, (5) Rubidium frequency standard, (6) Tube linking a turbomolecular pump to the microwave resonator,
(7) Helium gas connection to cryostat, (8) Liquid helium Dewar, (9) Thermostated chamber for pressure reading, regulation and control.

C. Measurement procedure

Prior to any experiment, to minimize the outgassing of impurities which might contaminate the helium, the resonator is maintained under high vacuum with a turbomolecular pump for at least a week at ambient temperature. The resonator, still under vacuum, is then cooled down to its operating temperature near 5 K, allowing time for thermal equilibration until the temperature is stable with a standard deviation of repeated measurements at the level of 50 μK. The resonance frequency of mode TM_{11} is measured first under vacuum, with a residual pressure below 10 µPa. The valve connecting the resonator to the turbomolecular pump is then closed and the pressure generator outlet-valve opened to fill the resonator with helium at the desired pressure. At each successive filling, the adiabatic heating due to compression alters the temperature stability of the gas within the resonator. Only once the pressure and temperature of the gas have recovered to acceptably stable conditions, are measurements of the resonance frequency under pressure carried out. Periodically, self-heating offsets of the thermometer readings are evaluated. Depending on the pressure range investigated, the evaluation of the pressure at the inlet of the cryostat may require a correction to account for the thermo-molecular effect. This effect, sometimes referred to as thermal transpiration, occurs when a rarefied gas (i.e. in the molecular flow regime) having a uniform pressure is subjected to a temperature gradient. A difference of pressure then arises between the warm and the cold parts of the gas enclosure[29]. It originates from the movement of molecules going from a higher density (colder) to a lower density (warmer) region of the gas. This process stops once the probabilities of forwards and backwards molecular movement equalize.

IV. EXPERIMENTAL RESULTS

In this section, we present and discuss the results of several tests of the metrological performance of the MRGM. These were performed to assess the resolution, precision, stability, and repeatability of microwave frequency measurements over several consecutive temperature runs between ambient temperature and 5 K (each identified by a chronological number) and pressure cycles in the range between vacuum and 20 kPa. We complete this discussion by presenting a detailed uncertainty budget of the microwave pressure standard.

In the following, we denote $f_{11,1}$, $f_{11,2}$ and $f_{11,3}$ the three single components of, for example, the TM_{11} microwave triplet, in ascending frequency order with respective half-widths $g_{11,1}$, $g_{11,2}$ and $g_{11,3}$.

A. Temperature dependence of microwave resonance frequencies

Whether the cavity is superconducting or not, the electromagnetic wave penetrates into the walls of the resonator, over a characteristic distance. The resonance frequency corresponds therefore to that of a sphere of slightly greater volume than that defined by the diameter of the cavity[21]. For a superconductor below its critical temperature T_c the temperature-dependent penetration depth λ(T) represents the penetration of an alternating magnetic field at the surface of the superconductor[30]. Figure 5 shows the amplitude of the measured transmission coefficient S_{21} of the central resonant frequency $f_{12,2}$ of the mode TM_{12} as a function of temperature when the cavity is progressively cooled from above to and below the

superconducting transition temperature of niobium at about 9.2 K. The peaks clearly sharpen for temperatures below 9.2 K.

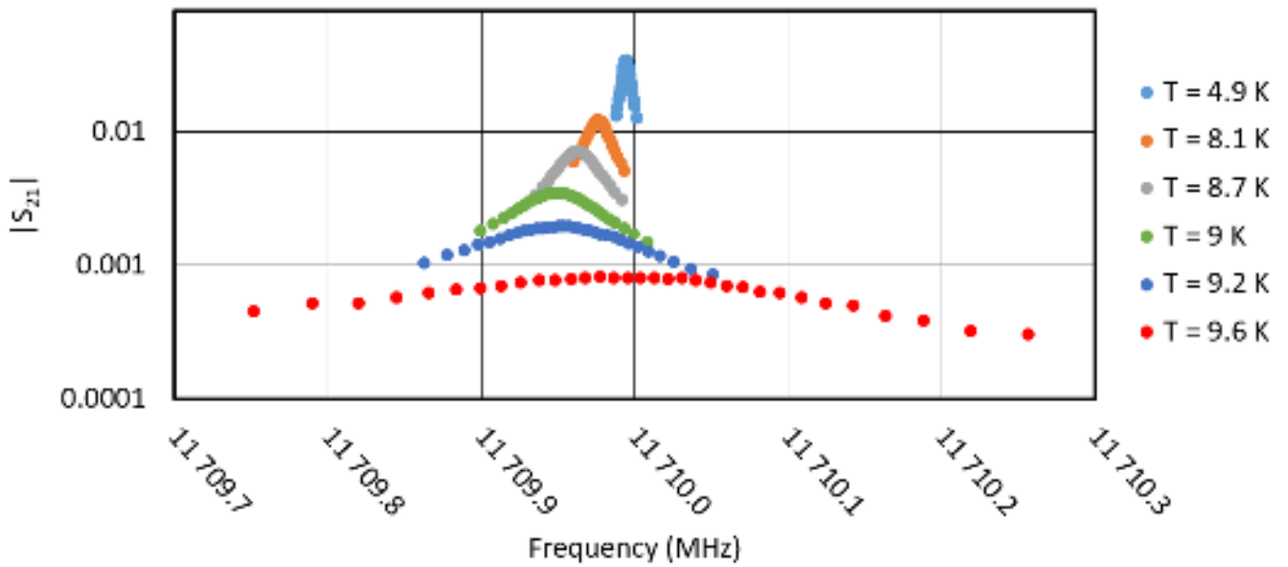

FIG. 5. Variation of the transmission coefficient | S_{21} | spectrum for resonant frequency $f_{12,2}$ of the mode TM_{12} at different temperatures.

B. Quality factor versus temperature

Since below its critical temperature, the surface resistance of the superconducting niobium coating is a function of temperature[30], the quality factor is also a function of temperature. Figure 6 shows the quality factors $Q_{11,1}$, $Q_{11,2}$ and $Q_{11,3}$ of the TM_{11} triplet components as a function of temperature. As expected for niobium, which is a type-II superconductor, they progressively increase as the temperature is lowered below the critical temperature T_c = 9.2 K and tend to become constant at low temperature[31,32]. Therefore, the lowest working temperatures correspond to the highest quality factors enhancing the resolution of frequency, and pressure measurements[18]. Following the test displayed in Figure 6, coupling to the cavity modes was reduced by reducing the insertion depth of the antennas, increasing the quality factor *Q* of the TM_{11} mode up to 3.8×10^6 at 5.4 K. Compared to a copper resonator the quality factor of a superconducting resonator is increased by a factor 100.

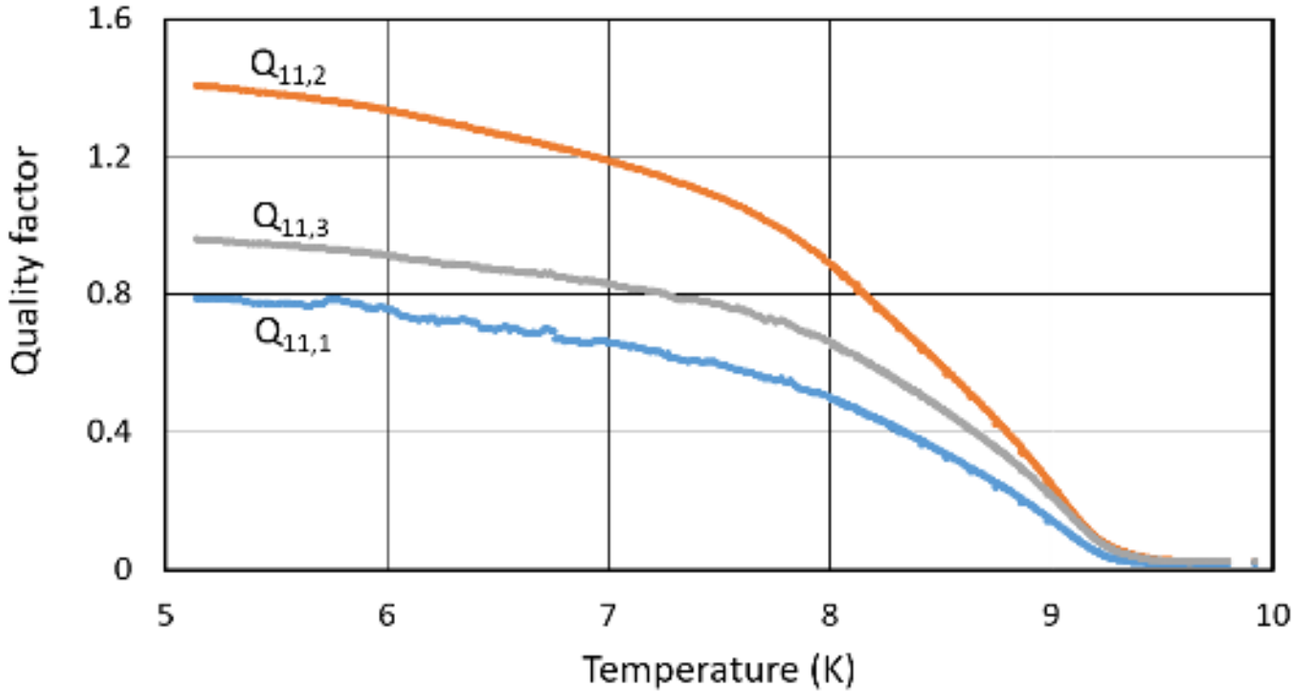

FIG. 6. Quality factors of the TM_{11} triplet resonant frequencies *versus* temperature measured under vacuum.

c. Relative frequency uncertainty

Figure 7 shows the relative uncertainty of a least-squares fit to the three single resonance frequencies composing the TM_{11} triplet, using a suitable function and a Levenberg-Marquardt[33,34] optimization algorithm, as in the procedure described in Ref.[21]. The measurements displayed in Figure 7 were recorded while the resonator was cooling down between 9.5 K and 5 K. It is evident that, within the triplet, the highest resonance frequency $f_{11,3}$ yields the lowest uncertainty. The points marked (1) and (2) correspond to measurements, in stable temperature conditions, of the relative uncertainty of the frequency $f_{11,3}$ at 5.1 K and 7.6 K. It is clear that the lowest uncertainty is obtained at the lowest temperature.

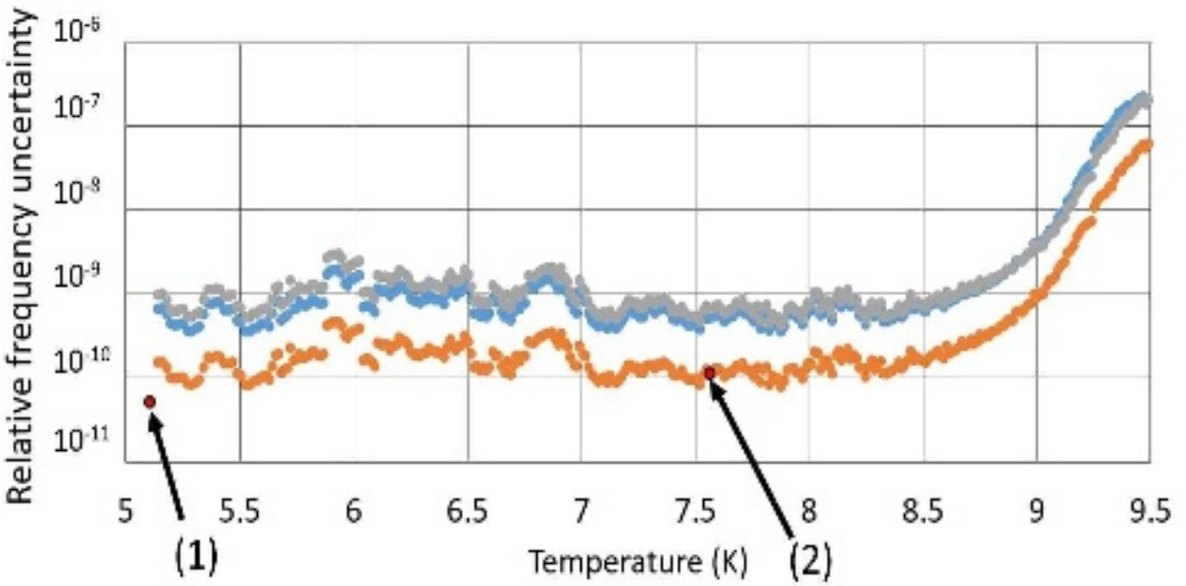

FIG. 7. Relative fitting uncertainty of the frequency of the TM_{11} mode triplet components *versus* temperature recorded while the resonator was rapidly cooling from 9.5 K to 5.1 K. Measurements in stable temperature conditions at (1) at 5.10 K and (2) 7.56 K.

D. Choice of the setpoint for the temperature regulation of the resonator

Tests conducted at different temperatures confirmed that the lowest uncertainty in the determination of the resonance frequency could be obtained near the lowest temperature achieved by the cryostat at about 4.7 K. Nevertheless, the set point temperature for all subsequent measurements and tests was fixed at 5.4 K, slightly above the critical point temperature of helium-4 at 5.2 K, to reduce the risk of insurgence of pre-condensation phenomena[35].

E. Stability under vacuum

The stability of resonance frequency measurement and the possible influence of undetected sources of noise or drifts was estimated by repeated measurements over two hours under vacuum at a temperature of 5.4 K.

Figure 8 shows the Allan deviation of this measurement series, with the slope marked −1/2 identifying the region where Gaussian noise is prevalent. In this region, the signal can be integrated to reduce the standard deviation of the mean, reducing the corresponding uncertainty contribution. After 85 s of integration time, the Allan deviation is 3×10^{-10}, corresponding to 15 mPa when converted into pressure; after 10 minutes of integration time, the Allan deviation reduces to 1×10^{-10}, equivalent to less than 6 mPa.

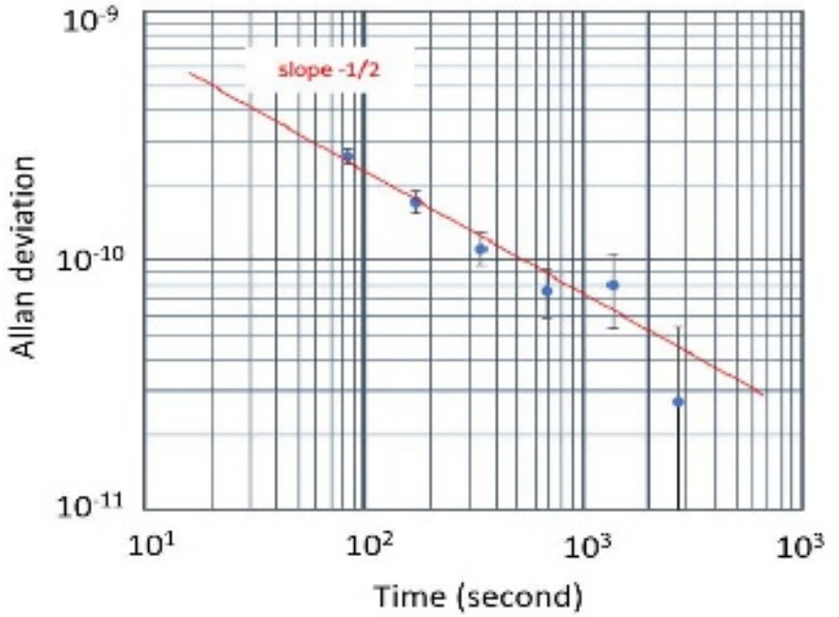

FIG. 8. Allan deviation of the resonant frequency with the resonator under vacuum at 5.4 K.

F. Experimental pressure resolution

The pressure resolution was estimated during the first tests. In the initial state, the resonator was under vacuum and at a temperature of 5.4 K. A helium pressure of 20 Pa was applied to it for about 45 min, at the end of which the gas was pumped out to restore the resonator to the initial state. As Figure 9 shows, a pressure variation of 20 Pa changes the resonant frequency by 2.5 kHz, while the fitting precision of the resonant frequency is about 0.27 Hz for TM_{11} mode. The frequency resolution of the present instrument corresponds to a pressure resolution of < 3 mPa.

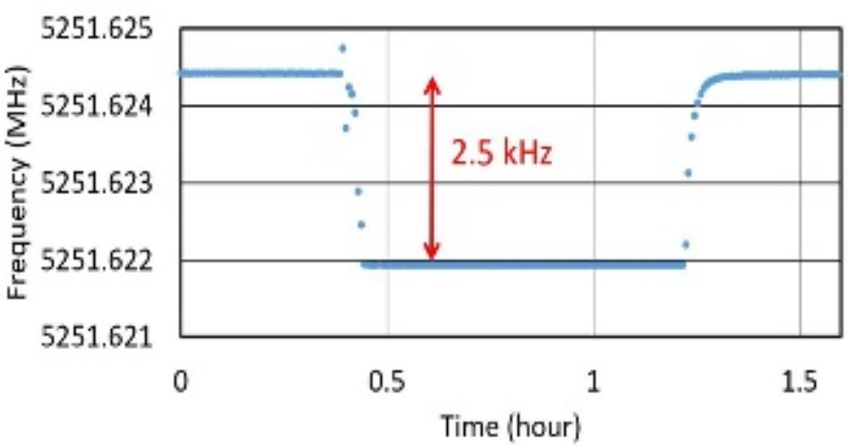

FIG. 9. Frequency shift induced by a 20 Pa variation of helium gas pressure at 5.4 K.

G. Pressure cycles

The temperature of the microwave resonator being regulated at 5.4 K, three series of measurements were performed varying the pressure between 20 kPa and 500 Pa in steps of 2 kPa. The pressure values were set, and the measurements were carried out automatically. Each step corresponds to about four hours of measuring time. Figure 10 shows pressure steps taken from a typical pressure cycle. Temperature spikes occur each time the pressure is changed because of adiabatic compression or expansion, and the time lapse needed to recover equilibrium by temperature regulation is around one hour.

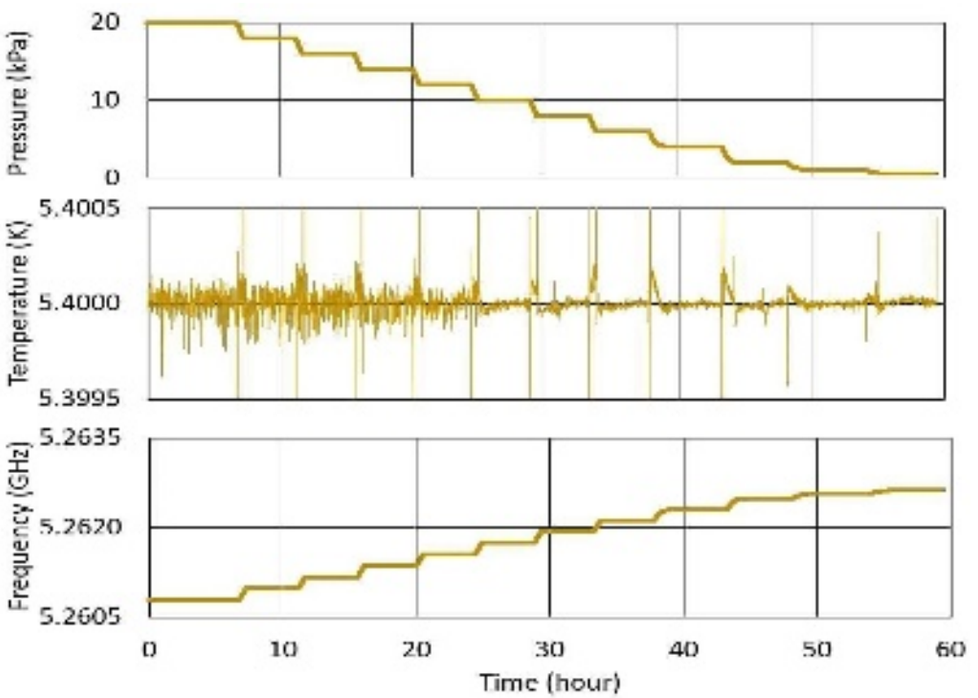

FIG. 10. Simultaneous evolution of the measured pressure (upper plot), resonator temperature (middle plot) and the resonant frequency of TM_{11} mode (lower plot) during a pressure cycle at a mean resonator temperature at 5.4 K.

Figure 11 shows the stability of the reference pressure around 20 kPa and the stability of temperature regulation at 5.4 K measured simultaneously over several hours.

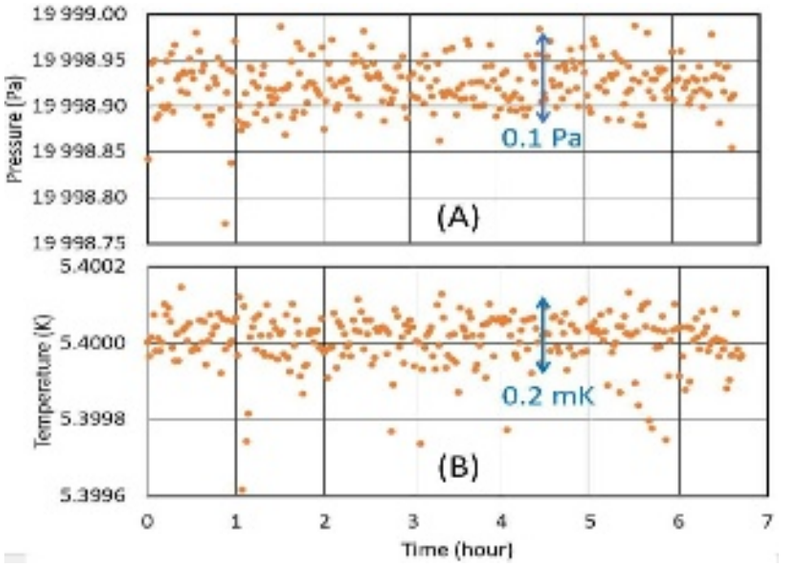

FIG. 11. Stability of the reference pressure (A) and the resonator temperature at 5.4 K (B) measured simultaneously.

Figures 12 to 14 show the relative and absolute differences between microwave pressure standard and a reference sensor, traceable to national standards, over three cycles carried out successively and identified by the numbers 1, 2 and 3. For the sake of comparison, the correction to account the thermomolecular effect was calculated following the recommendation of guide to the realization of the ITS-90 was used[36].

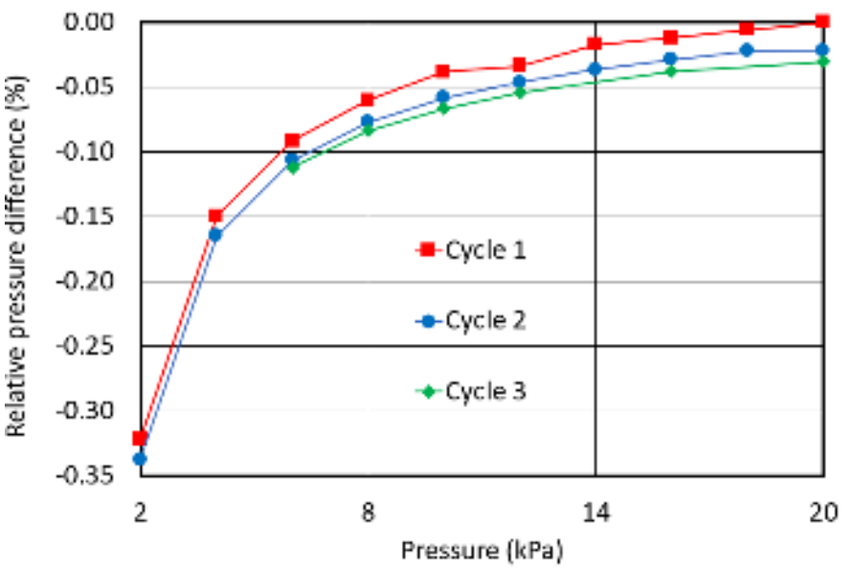

FIG. 12. Relative pressure difference $\Delta p/p = (p_{MRGM} - p_{ref}/p)$ between the microwave manometer and a calibrated reference pressure transducer for three successive cycles where the pressure was stepped down from 20 kPa to 2 kPa.

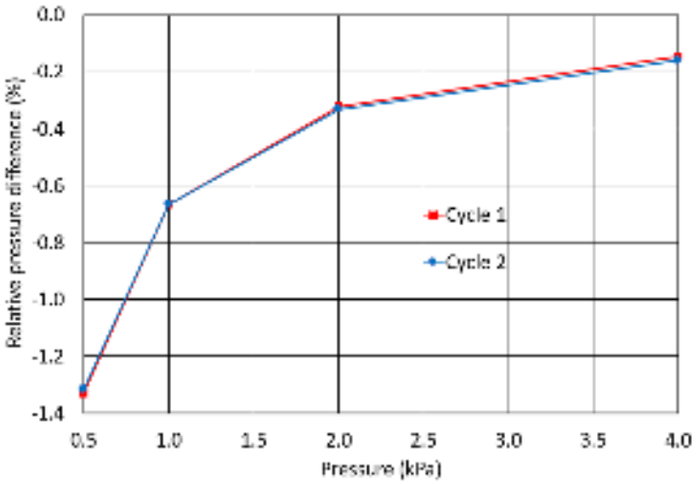

FIG. 13. Relative pressure difference $\Delta p/p = (p_{MRGM} - p_{ref}/p)$ between the microwave manometer and a calibrated reference pressure transducer for the first two successive cycles between 4 kPa and 500 Pa. The last cycle could not be completed due to a lack of liquid helium.

Figure 14 shows that the results obtained over subsequent pressure cycles are not reproducible with the difference between the microwave standard and the reference sensor increasing at low pressure.

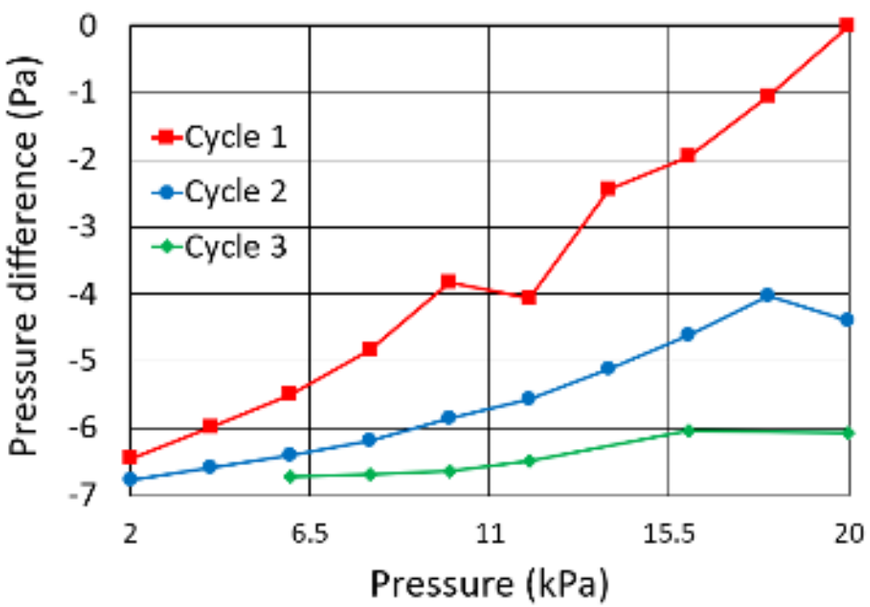

FIG. 14. Absolute difference $\Delta p = (p_{MRGM} - p_{ref})$ between the microwave manometer and a calibrated reference pressure transducer for three successive cycles where the pressure was stepped down from 20 kPa to 2 kPa.

As a possible justification for the unsatisfactory repeatability, we observe that the stability of the 8.5-digit multimeter used to measure the temperature of the resonator was inadequate, being heavily affected by ambient temperature variations, and presumably drifting over several weeks of measuring time. Regarding the difference between the MRGM and the reference pressure sensor, which increases at low pressure, we suppose that the thermo-molecular pressure correction used is not adequate to account for some defects of the present cryostat. It is possible that traces of glue or soldering tin in the pressure tube at the inlet of the cryostat increase the thermo-molecular effect in a way difficult to estimate. We anticipate that a future improved apparatus will allow the measurement of this effect *in situ* to quantify this correction with greater confidence.

H. Provisional uncertainty budget

Table I shows the provisional uncertainty budget of the microwave sensor for helium pressure of 500 Pa and 20 kPa, with the superconducting resonator temperature at 5.4 K. The listed uncertainties were determined by the 'Influence Coefficient method[37] by evaluating the contribution of each factor on the measured pressure by iterative calculation from their physical expressions. Uncertainty estimates attributed to the temperature reference thermometer correspond to their calibration uncertainty. The temperature control uncertainty 'T regulation' is evaluated from experimental runs. The relative uncertainty estimate for the isothermal compressibility κ_T is 1% as from Ref[22]. The uncertainties of the *ab initio* coefficients A_μ, A_ε, B_ε, B_ρ, C_ρ and D_ρ are interpolated, at the working temperature, from published estimates of *ab initio* calculations[14,38]. The frequency uncertainties 'fm measurement and corrections' includes contributions from fitting, microwave instrumentation, and corrections for thermal expansion.

The prevalent uncertainty contributions are from the temperature measurements and from the poor repeatability which is apparent from the scatter of frequency results over repeated measurement cycles. We remark that, for future work, the use of a rhodium-iron standard thermometer calibrated against an acoustic gas thermometer (AGT) would reduce the uncertainty contribution of temperature measurement by a factor of 21 with the combined uncertainty of the standard becoming 28 mPa (53 ppm) at 500 Pa and about 1900 mPa (97 ppm) at 20 kPa.

The search for a possible explanation of the poor repeatability of microwave frequency measurements over repeated measurement cycles stimulated several tests, including: a verification of the influence of an external magnetic field on the measured resonance frequency, with the apparatus being tested with and without then an anti-magnetic shielding in place; several reference oscillators (10 MHz) were tested, including a rubidium frequency standard, and a GPS reference to achieve better long-term stability; the vector network analyzer used to measure resonant frequency was serviced and had a new calibration; the resonator temperature measurement uncertainty was checked by temporarily using a high-performance resistance bridge; microwave acquisition and curve fitting algorithms were improved and different types of low-noise amplifiers, microwave isolators and antennas were tested; the position and type of control thermometer were varied; the closure of the resonator hemispheres was refined; heater positions were modified. Finally, tests were also performed using argon gas instead of helium, at the temperature of the triple point of argon (≈ 83.8 K), to assess the possible influence of pre-condensation effects.

Despite all these tests, a convincing explanation of repeatability issues still requires further investigation.

V. CONCLUSION

TABLE I. Helium gas pressure measurement uncertainty budget for a superconducting microwave cavity at T=5.4 K. Key: P pressure; κ_T isothermal compressibility; T thermodynamic temperature; A_μ molar magnetic polarizability; A_ε molar electric polarizability; B_ε second dielectric virial coefficient; B_ρ, C_ρ, D_ρ density virial coefficients; f_m measured frequency. Uncertainty components less than 20 μPa are either omitted or replaced by a dash – .

Working pressure	500 Pa	20 kPa
Uncertainty unit	(mP)	(mPa)
p uncertainty components, Type B		
κ_T	0.7	26
T calibration	200	7900
Gas impurities	–	–
$A_\mu{}^{20}$	0.2	6
$A_\varepsilon{}^{15}$	0.1	4
$B_\varepsilon{}^{15}$	0.06	36
$B_\rho{}^{38}$	0.06	47
$C_\rho{}^{38}$	–	7
$D_\rho{}^{38}$	–	1
p uncertainty components, Type A		
T regulation	7	49
Repeatability	20	1900
f_m measurement and corrections	16	136
***p* combined uncertainty**	**200**	**8100**

V. CONCLUSION

We have described a primary pressure standard for the range 500 Pa to 20 kPa aimed at providing better calibration and measurement capabilities in this range than those currently available using pressure balances. In the present work, pressure is measured via refractive index gas manometry using helium-4. The refractive index is measured using microwave resonance (from 5.0 GHz to 11.7 GHz) with a quasispherical niobium-coated copper resonator. As far as we are aware, this is the first time a superconducting microwave cavity has been used to measure pressure. This proof-of-principle study is

complementary to work using argon gas in a (non-superconducting) copper microwave resonator, whose performance is currently under evaluation.

A preliminary uncertainty evaluation of the microwave pressure standard presented here yields a standard uncertainty of 0.2 Pa at 500 Pa and 8.2 Pa at 20 kPa, with a major contribution from thermometry which might be substantially reduced in future work, using a rhodium-iron thermometer directly calibrated on the thermodynamic temperature scale, *e.g.* by acoustic gas thermometry[7], and a resistance bridge to increase measurement repeatability. At 20 kPa roughly half of the present uncertainty arises from the limited repeatability of the measurements reported here, whose origin requires further investigation.

ACKNOWLEDGMENTS

The authors thank Dr Robert F. Berg of NIST for his kind reading of the manuscript and Dr. James W. Schmidt of NIST for his helpful discussions. This project (18SIB04 QuantumPascal) has received funding from the EMPIR programme co-financed by the Participating States and from the European Union's Horizon 2020 research and innovation programme.

REFERENCES

[1]M.R. Moldover. Can a pressure standard be based on capacitance measurements? *Journal of Research of the National Institute of Standards and Technology*, 103(2):167, 1998.

[2]J. J. Hurly and M. R. Moldover. Ab initio values of the thermophysical properties of helium as standards. *J. Res. Natl. Inst. Stand. Tech.*, 105(5):667–688, 2000.

[3]M. Puchalski, K. Szalewicz, M. Lesiuk, and B. Jeziorski. Qed calculation of the dipole polarizability of helium atom. *Phys. Rev. A*, 101(2):022505, 2020.

[4]P. Czachorowski, M. Przybytek, M. Lesiuk, M. Puchalski, and B. Jeziorski. Second virial coefficients for he 4 and he 3 from an accurate relativistic interaction potential. *Phys. Rev. A*, 102(4):042810, 2020.

[5]G. Garberoglio and A. H. Harvey. Path-integral calculation of the second dielectric and refractivity virial coefficients of helium, neon, and argon. *J. Res. Natl. Inst. Stand. Technol.*, 125, 2020.

[6]R. Hellmann, C. Gaiser, B. Fellmuth, T. Vasyltsova, and E. Bich. Thermophysical properties of low-density neon gas from highly accurate firstprinciples calculations and dielectric-constant gas thermometry measurements. *J. Chem. Phys.*, 2021.

[7]M. R. Moldover, R. M. Gavioso, J. B. Mehl, L. Pitre, M. de Podesta, and J.T. Zhang. Acoustic gas thermometry. *Metrologia*, 51(1):R1–R19, 2014.

[8]R. Hellmann. Ab initio potential energy surface for the nitrogen molecule pair and thermophysical properties of nitrogen gas. *Mol. Phys.*, 111(3):387– 401, 2013.

[9]L.R. Pendrill. Macroscopic and microscopic polarizabilities of helium gas. *J. Phys. B: At. Mol. Opt. Phys.*, 1996.

[10]H. Fang and P. Juncar. A new simple compact refractometer applied to measurements of air density fluctuations. *Rev. Sci. Instrum.*, 70(7):3160– 3166, 1999.

[11]K. Jousten, J. Hendricks, D. Barker, K. Douglas, S. Eckel, P. Egan, J. Fedchak, J. Flügge, C. Gaiser, D. Olson, J. Ricker, T. Rubin, W. Sabuga, J. Scherschligt, R. Schöde, U. Sterr, J. Stone, and G. Strouse. Perspectives for a new realization of the pascal by optical methods. *Metrologia*, 54(6):s146, 2017.

[12]P. F. Egan, J. A. Stone, J. H. Hendricks, J. E. Ricker, G. E. Scace, and G. F. Strouse. Performance of a dual fabry–perot cavity refractometer. *Opt. Lett.*, 40(17):3945–3948, 2015.

[13]P. F. Egan, J. A. Stone, J. E. Ricker, and J. H. Hendricks. Comparison measurements of low-pressure between a laser refractometer and ultrasonic manometer. *Rev. Sci. Instr.*, 84(5):053113, 2016.

[14]P. M. C. Rourke, C. Gaiser, B. Gao, D. Madonna Ripa, M. R. Moldover, L. Pitre, and R. J. Underwood. Refractive-index gas thermometry. *Metrologia*, 2019.

[15]J.W. Schmidt, R.M. Gavioso, E.F. May, and M.R. Moldover. Polarizability of helium and gas metrology. *Phys. Rev. Lett.*, 98(25):254504, 2007.

[16]C. Gaiser, B. Fellmuth, and W. Sabuga. Primary gas-pressure standard from electrical measurements and thermophysical ab initio calculations. *Nat. Phys.*, 16(2):177–180, 2020.

[17]C. Gaiser, B. Fellmuth, and W. Sabuga. Primary gas pressure standard passes next stress test. *Ann. Phys.*, page 2200336, 2022.

[18]B. Gao, L. Pitre, E.C. Luo, M.D. Plimmer, P. Lin, J.T. Zhang, X.J. Feng, Y.Y. Chen, and F. Sparasci. Feasibility of primary thermometry using refractive index measurements at a single pressure. *Measurement*, 103:258– 262, 2017.

[19] P.J. Mohr, D.B. Newell, B.N. Taylor and E. Tiesinga. Data and analysis for the CODATA 2017 special fundamental constants adjustment. *Metrologia* 55: 125–46, 2018

[20]P.M.C. Rourke. Perspective on the refractive-index gas thermometry data landscape. *J. Phys. Chem. Ref. Data*, 50(3):033104, 2021.

[21]E.F. May, L. Pitre, J. B. Mehl, M. R. Moldover, and J. W. Schmidt. Quasispherical cavity resonators for metrology based on the relative dielectric permittivity of gases. *Rev. Sci. Instrum.*, 75:3307–3317, 2004.

[22]N.J. Simon, E.S. Drexler, and R.P. Reed. *Properties of Copper and Copper Alloys at Cryogenic Temperatures*, volume 177 of *NIST Monograph*. National Institute of Standards and Technology, 1992.

[23]S.R. Stein and J.P. Turneaure. Superconducting resonators: High stability oscillators and applications to fundamental physics and metrology. In *AIP Conference Proceedings*, volume 44, pages 192–213. American Institute of Physics, 1978.

[24]L. Pitre, F. Sparasci, L. Risegari, C. Guianvarc'h, C. Martin, M.E. Himbert, M.D. Plimmer, A. Allard, B. Marty, P.A. Giuliano Albo, et al. New measurement of the boltzmann constant k by acoustic thermometry of helium-4 gas. *Metrologia*, 2017.

[25]J. B. Mehl, M. R. Moldover, and L. Pitre. Designing quasi-spherical resonators for acoustic thermometry. *Metrologia*, 41(4):295–304, June 2004.

[26]S. Bauer, W. Diete, B. Griep, M. Peiniger, H. Vogel, P. vom Stein, S. Calatroni, E. Chiaveri, and R. Losito. Production of nb/cu sputtered superconducting cavities for lhc. In *Proc. 9th Workshop on RF Superconductivity, Santa Fe, New Mexico, USA*, 1999.

[27]P. Gambette. *Towards a quantum standard for absolute pressure measurements*. PhD thesis, HESAM Université France, 2021.

[28]To accurately describe the experimental setup and procedures used, it may be necessary to identify commercial products by their manufacturers' names or labels. However, this identification does not imply endorsement by LNE-Cnam or INRiM, nor does it mean that the specific product or equipment is necessarily the best available option for the intended purpose.

[29]C. M. Rojas, I. Graur, P. Perrier, and J. G. Meolans. Thermal transpiration flow: A circular cross-section microtube submitted to a temperature gradient. *Physics of Fluids*, 23(3):031702, 2011.

[30]H. Padamsee. *RF Superconductivity Science, Technology and Applications*. Wiley Online Library, 2009.

[31]D.K. Finnemore, T.F. Stromberg, and C.A. Swenson. Superconducting properties of high-purity niobium. *Physical Review*, 149(1):231, 1966.

[32]L. Frunzio, A. Wallraff, D. Schuster, J. Majer, and R. Schoelkopf. Fabrication and characterization of superconducting circuit QED devices for quantum computation. *IEEE Trans. Appl. Supercond.*, 15(2):860–863, 2005.

[33]K. Levenberg. A method for the solution of certain non-linear problems in least squares. *Quarterly of applied mathematics*, 2(2):164–168, 1944.

[34]D. W. Marquardt. An algorithm for least-squares estimation of nonlinear parameters. *Journal of the society for Industrial and Applied Mathematics*, 11(2):431–441, 1963.

[35]J. B. Mehl and M. R. Moldover. Precondensation phenomena in acoustic measurements. *J. Chem. Phys.*, 77(1):455–465, 1982.

[36]BIPM. Guide to the realization of the ITS-90 - Interpolating ConstantVolume Gas Thermometry, 2018.

[37]O.F. Smidts and J. Devooght. A variational method for determining uncertain parameters and geometry in hydrogeology. *Reliability Engineering & System Safety*, 57(1):5–19, 1997.

[38]K. R. S. Shaul, A. J. Schultz, and D. A. Kofke. Path-integral Mayersampling calculations of the quantum Boltzmann contribution to virial coefficients of Helium-4. *J. Chem. Phys.*, 137(18):184101, November 2012.


A


B

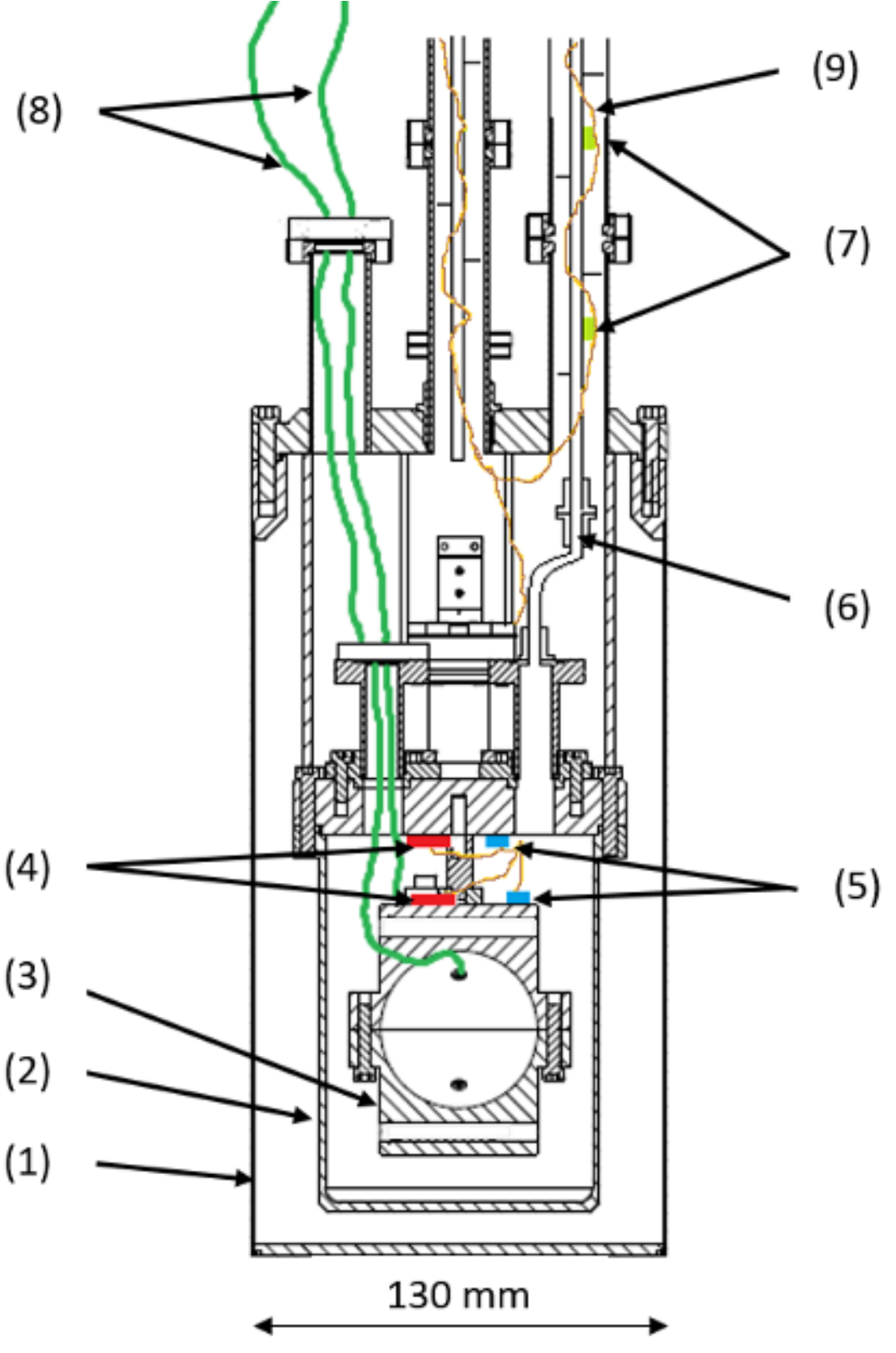
(8)
(9)
(7)
(6)
(4)
(5)
(3)
(2)
(1)
130 mm

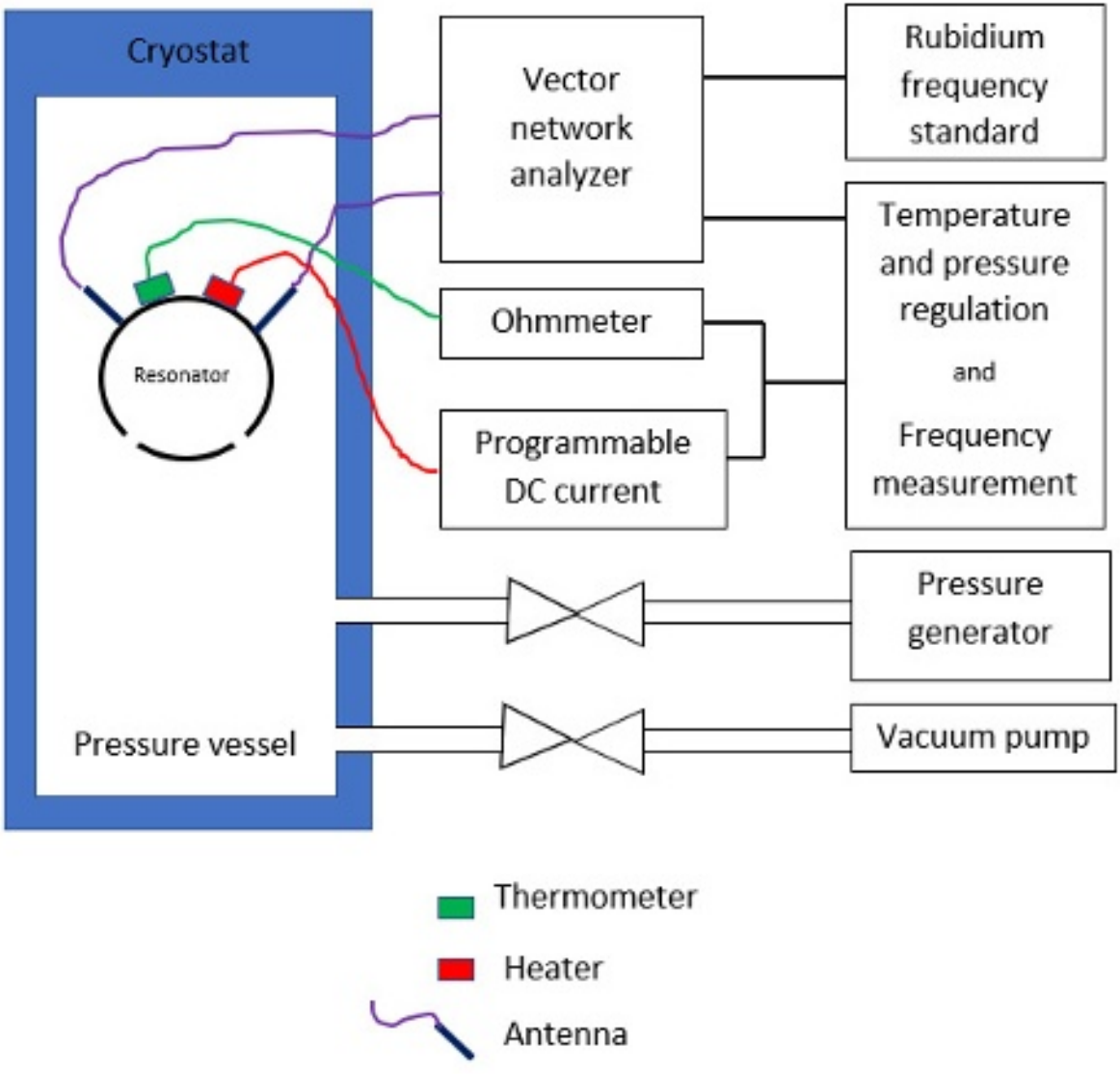
Cryostat
Resonator
Pressure vessel
Vector network analyzer
Ohmmeter
Programmable DC current
Rubidium frequency standard
Temperature and pressure regulation
and
Frequency measurement
Pressure generator
Vacuum pump
Thermometer
Heater
Antenna

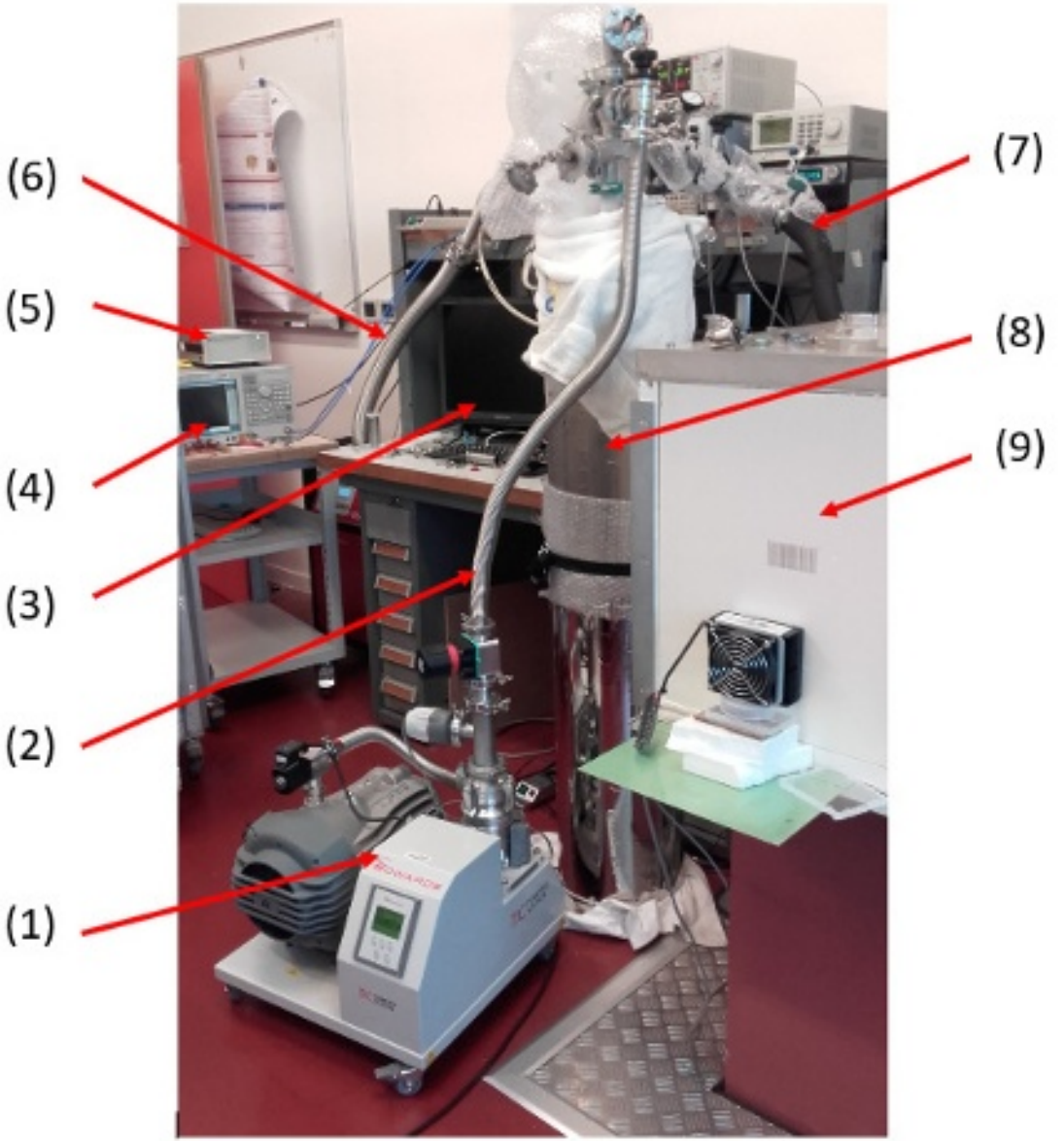
(6)
(5)
(4)
(3)
(2)
(1)
(7)
(8)
(9)

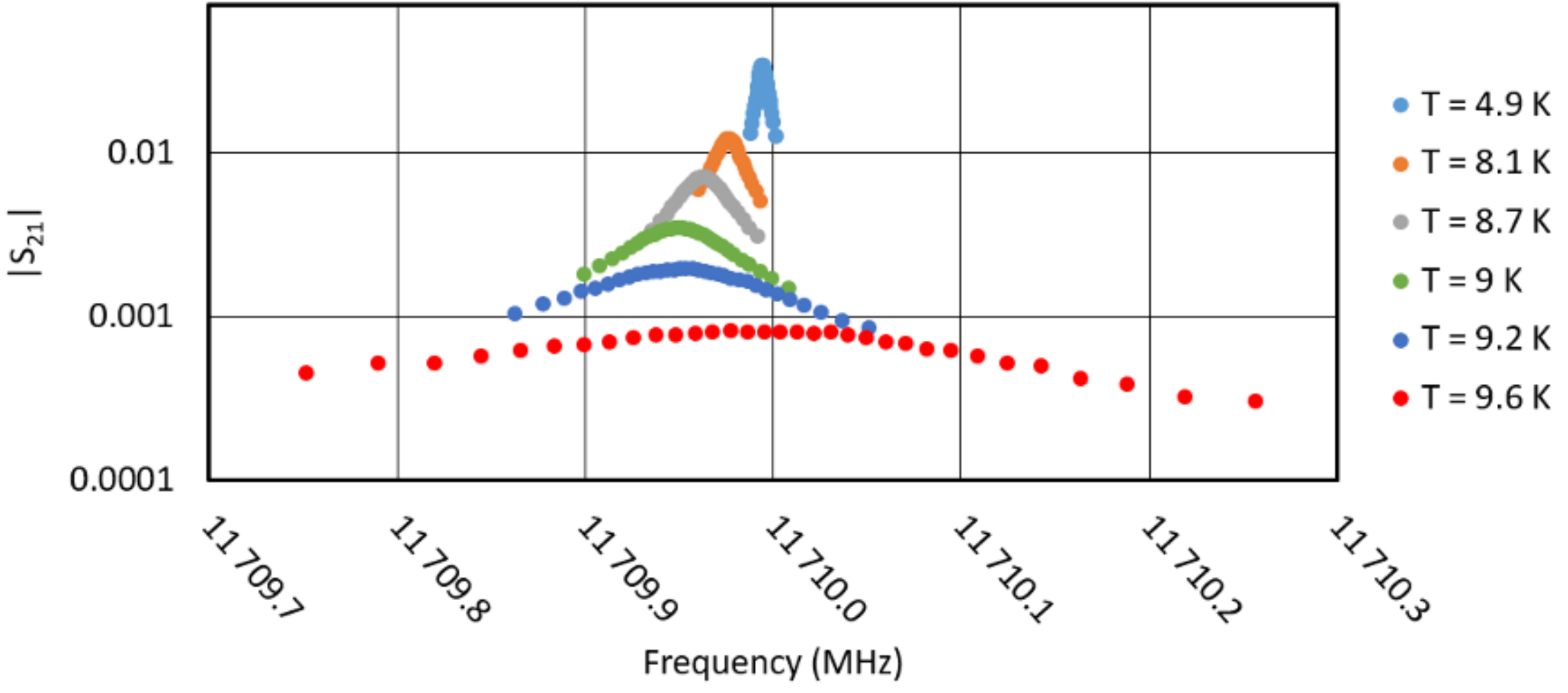
0.01
0.001
0.0001
|S21|
11 709.7
11 709.8
11 709.9
11 710.0
11 710.1
11 710.2
11 710.3
Frequency (MHz)
T = 4.9 K
T = 8.1 K
T = 8.7 K
T = 9 K
T = 9.2 K
T = 9.6 K

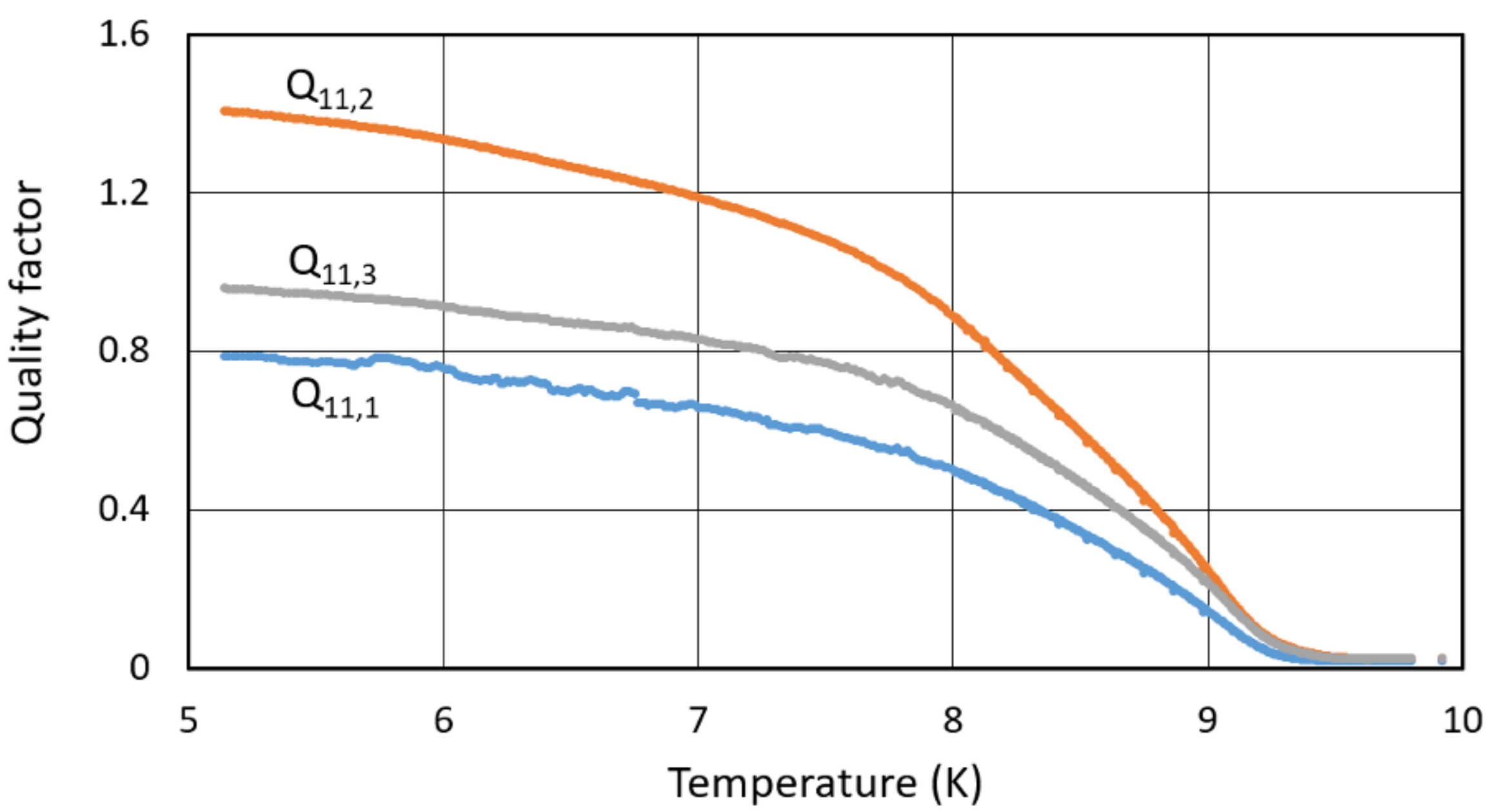
1.6
1.2
0.8
0.4
0
Quality factor
$Q_{11,2}$
$Q_{11,3}$
$Q_{11,1}$
5
6
7
8
9
10
Temperature (K)

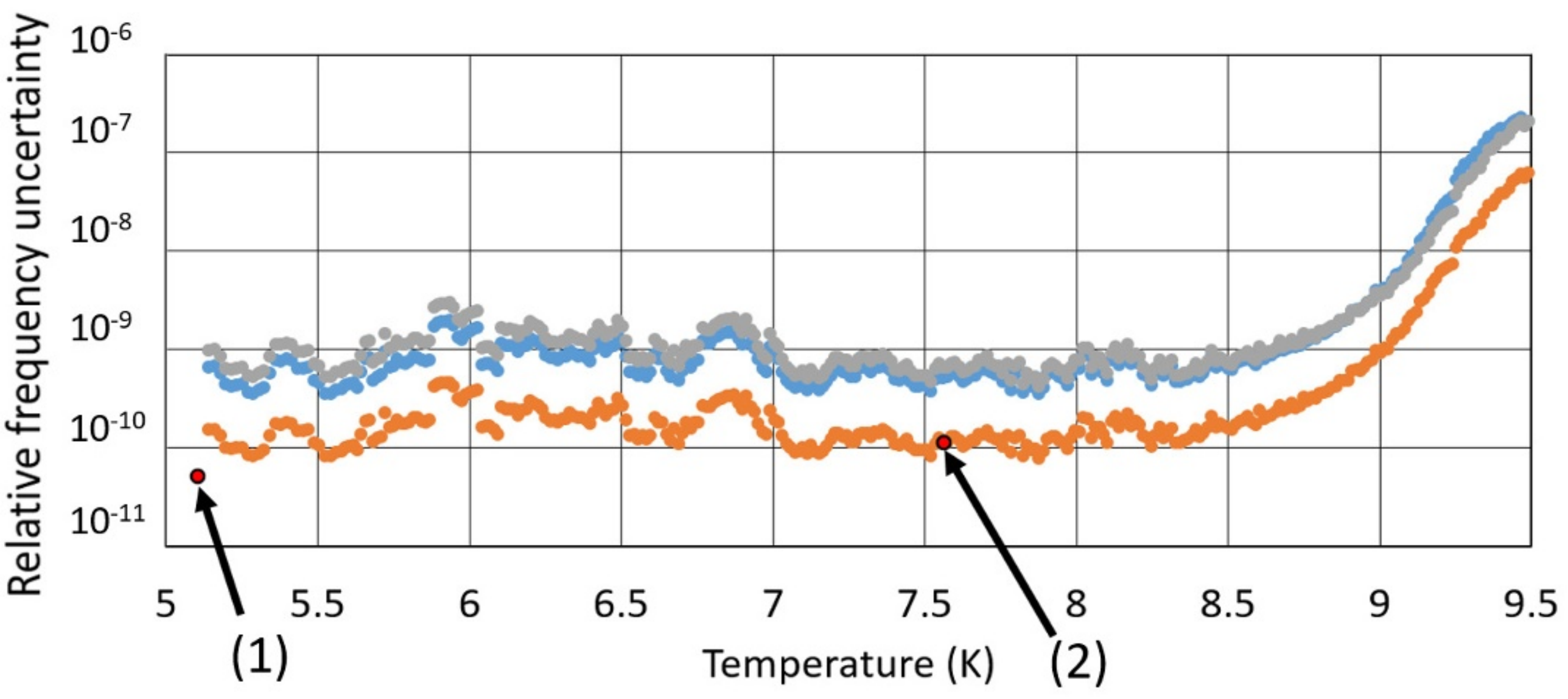
Relative frequency uncertainty
10-6
10-7
10-8
10-9
10-10
10-11
5
5.5
6
6.5
7
7.5
8
8.5
9
9.5
Temperature (K)
(1)
(2)

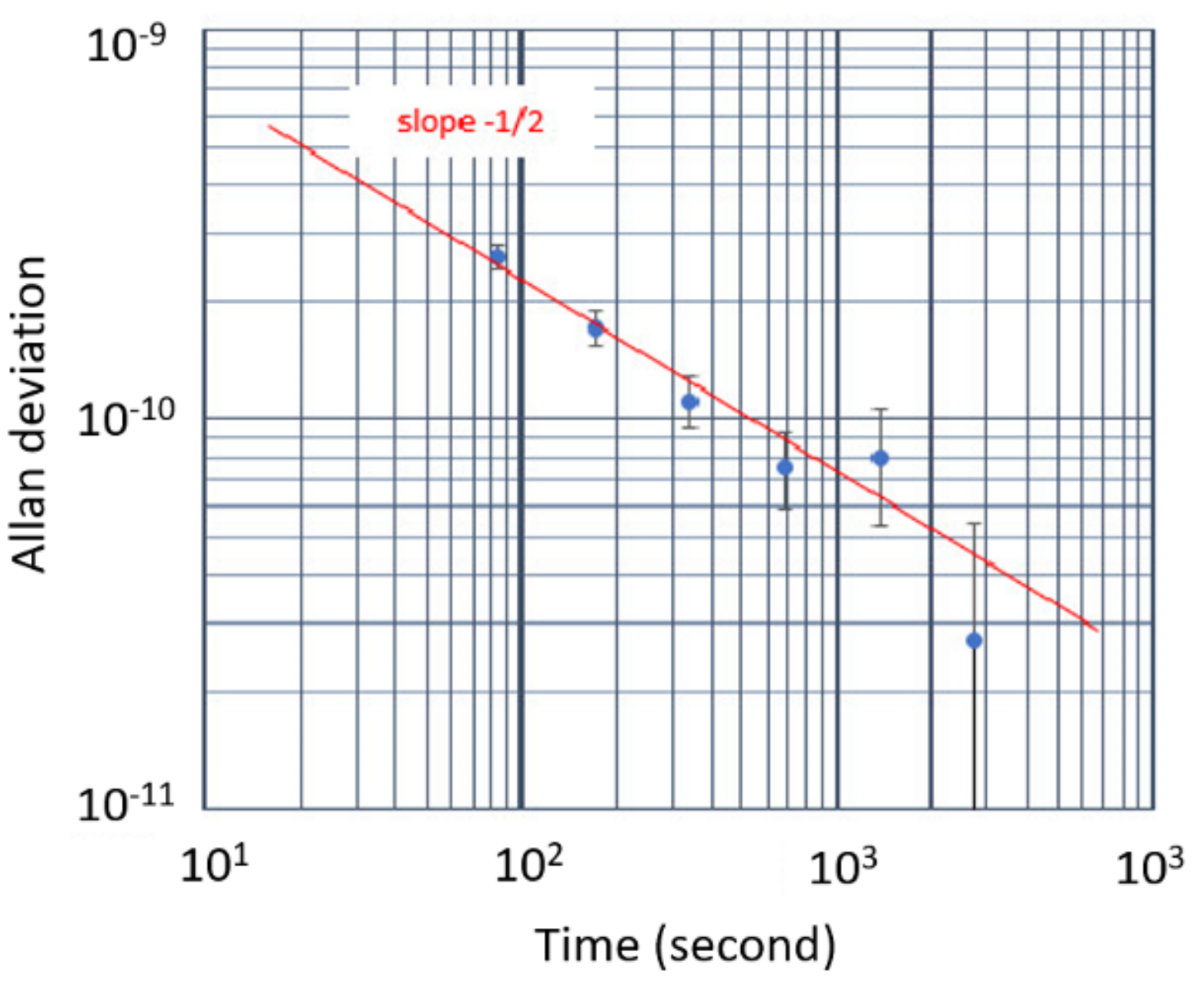
slope -1/2
Allan deviation
10^{-9}
10^{-10}
10^{-11}
10^{1}
10^{2}
10^{3}
10^{3}
Time (second)

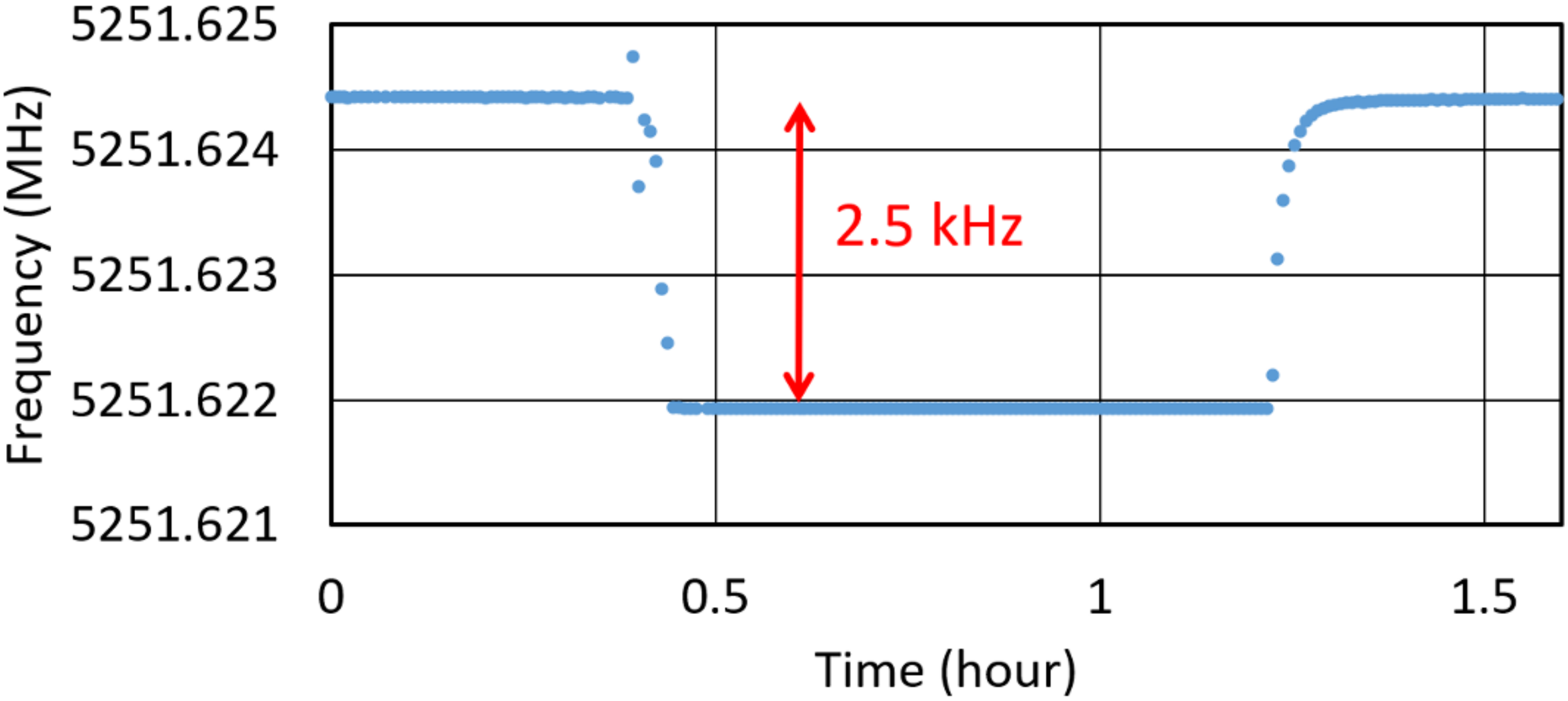
5251.625
5251.624
5251.623
5251.622
5251.621
Frequency (MHz)
2.5 kHz
0
0.5
1
1.5
Time (hour)

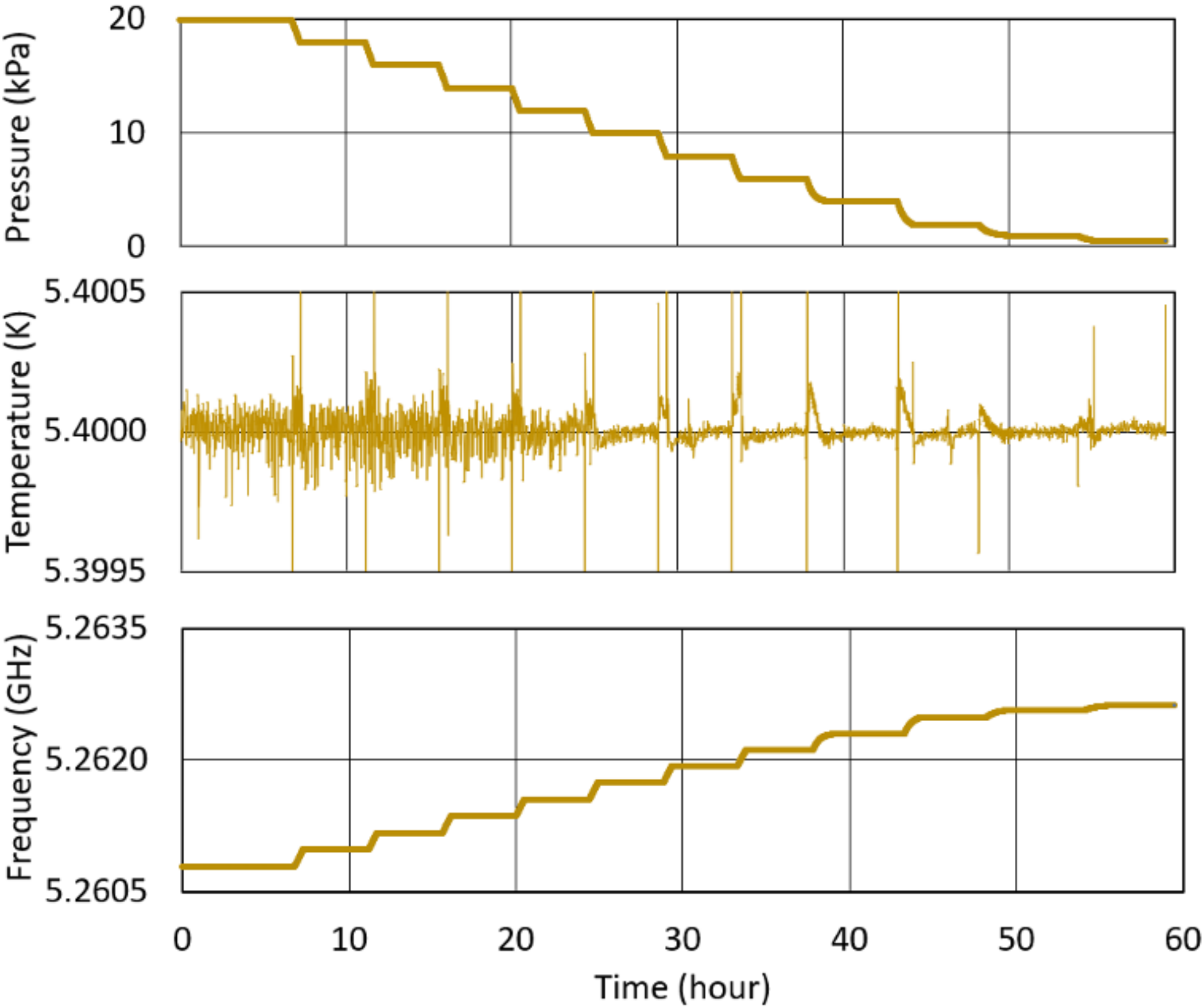
Pressure (kPa)
20
10
0
Temperature (K)
5.4005
5.4000
5.3995
Frequency (GHz)
5.2635
5.2620
5.2605
0
10
20
30
40
50
60
Time (hour)

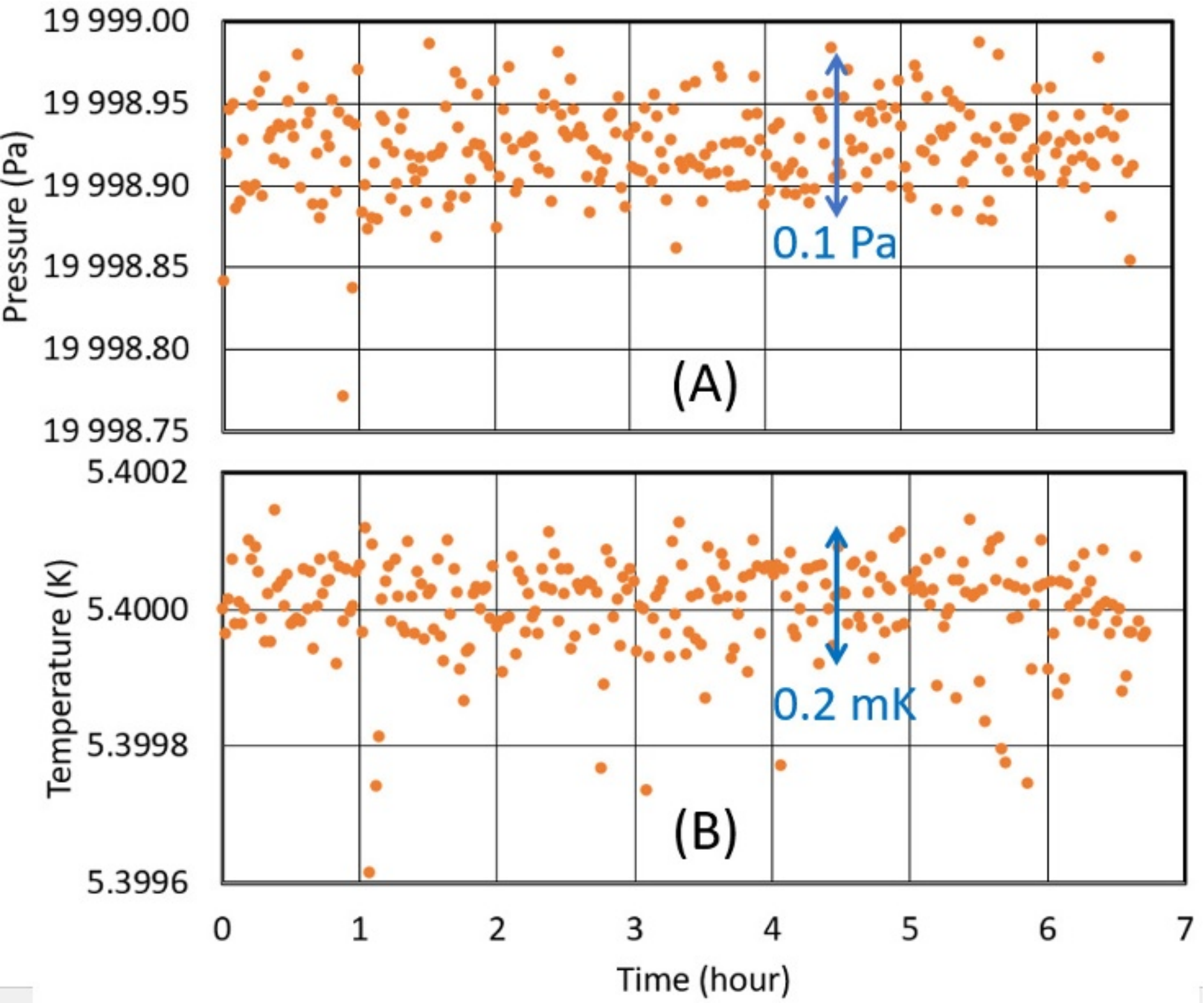
19 999.00
19 998.95
19 998.90
19 998.85
19 998.80
19 998.75
Pressure (Pa)
0.1 Pa
(A)
5.4002
5.4000
5.3998
5.3996
Temperature (K)
0.2 mK
(B)
0
1
2
3
4
5
6
7
Time (hour)

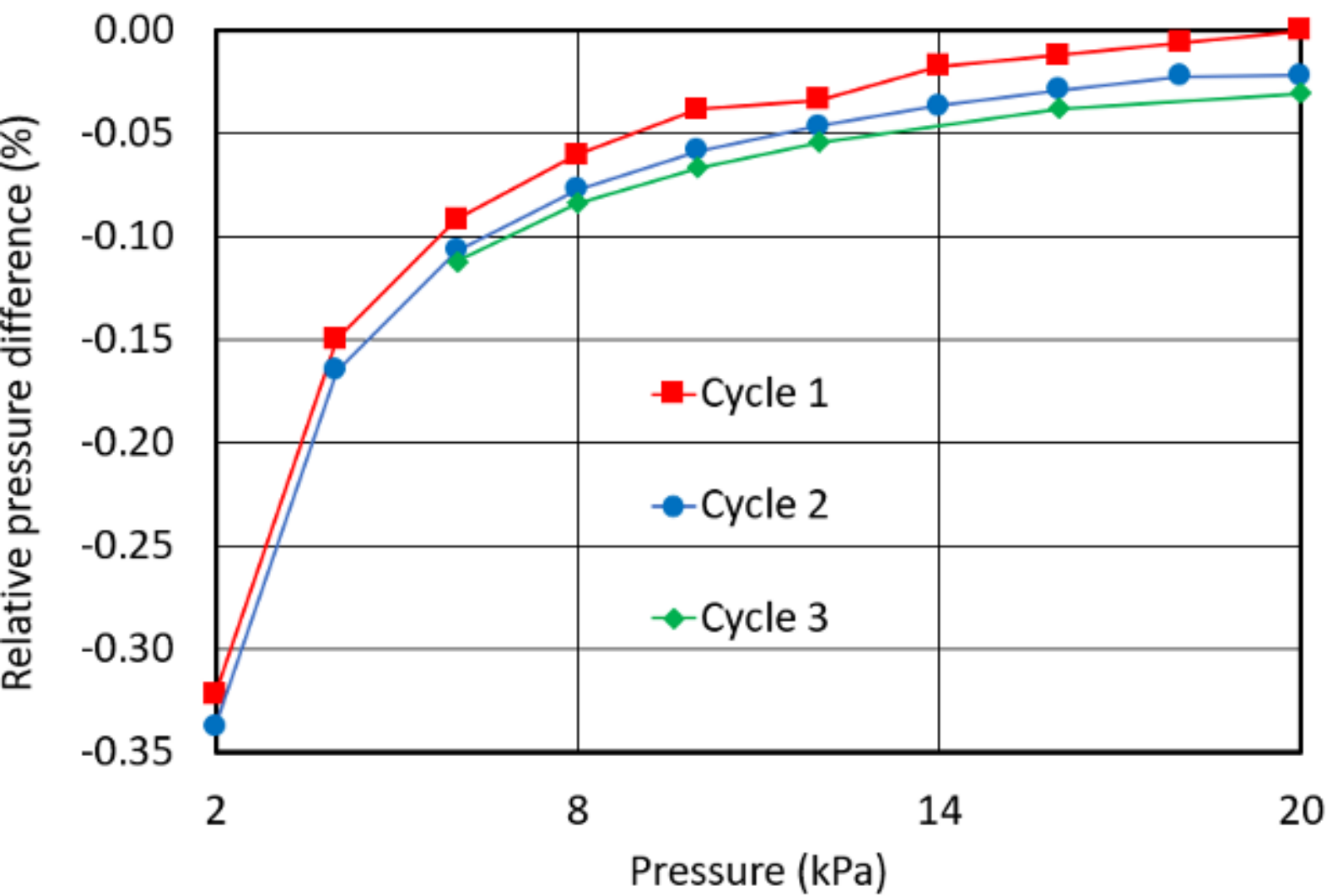
0.00
-0.05
-0.10
-0.15
-0.20
-0.25
-0.30
-0.35
Relative pressure difference (%)
2
8
14
20
Pressure (kPa)
Cycle 1
Cycle 2
Cycle 3

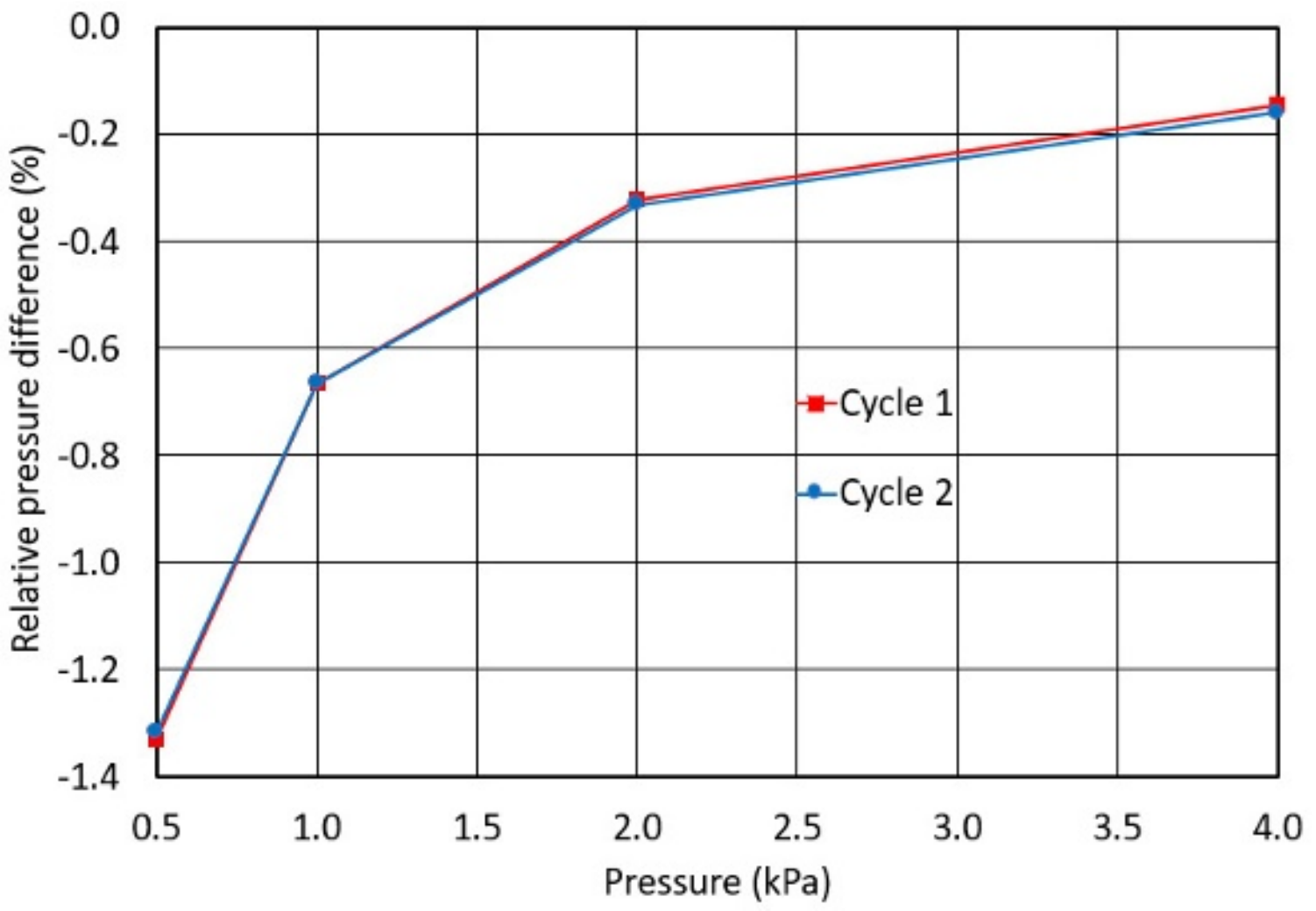
0.0
-0.2
-0.4
-0.6
-0.8
-1.0
-1.2
-1.4
Relative pressure difference (%)
0.5
1.0
1.5
2.0
2.5
3.0
3.5
4.0
Pressure (kPa)
Cycle 1
Cycle 2

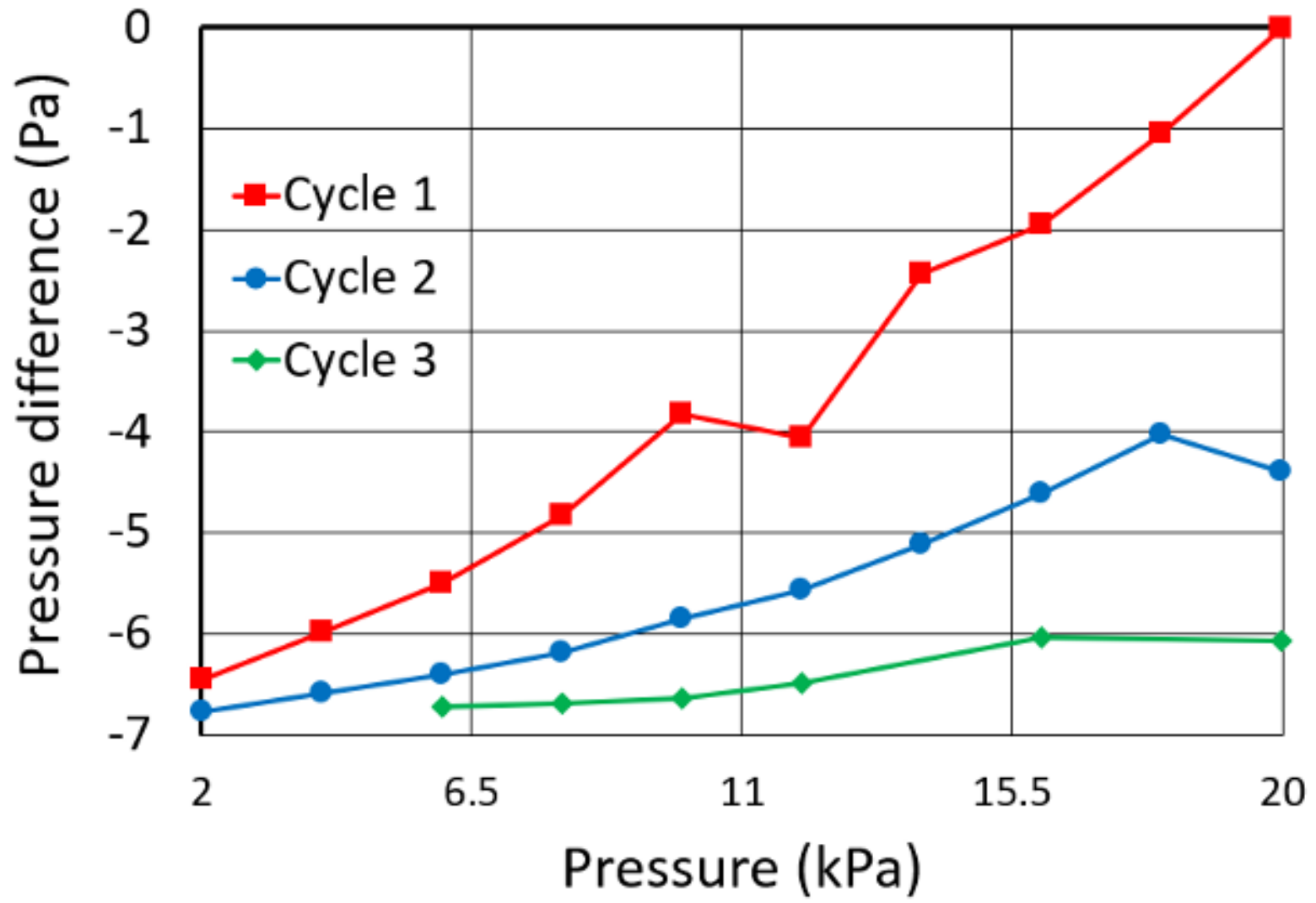
Pressure difference (Pa)
0
-1
-2
-3
-4
-5
-6
-7
Cycle 1
Cycle 2
Cycle 3
2
6.5
11
15.5
20
Pressure (kPa)